

# LIDDICOATITE TOURMALINE FROM ANJANABONOINA, MADAGASCAR

By Dona M. Dirlam, Brendan M. Laurs, Federico Pezzotta, and William B. (Skip) Simmons

Liddicoatite, a calcium-rich lithium tourmaline, was recognized as a separate mineral species in 1977, and named in honor of Richard T. Liddicoat. Most of the remarkable polychrome tourmalines with varied geometric patterns that are characteristic of this species were produced during the 20th century from the Anjanabonoina pegmatite deposit in central Madagascar. To best display its complex color zoning and patterns, the tourmaline is commonly sold as polished slices or carvings. Liddicoatite exhibits physical and optical properties that overlap those of elbaite, so quantitative chemical analysis is required to distinguish these species; both may occur in a single crystal. The most common internal features are color zoning, strain patterns, partially healed fractures, feathers, needle-like tubes, negative crystals, and albite inclusions.

For decades, liddicoatite from Madagascar has been prized for its dramatic color zoning. Among the myriad geometric patterns displayed in polychrome slices cut perpendicular to the c-axis (figure 1), triangular zones and three-rayed “stars” resembling a Mercedes Benz symbol are the most recognizable features of this remarkable tourmaline. The diversity of colors and patterns shown by Madagascar liddicoatite has not been seen in tourmaline from other localities. The Anjanabonoina pegmatite deposit in central Madagascar is one of the world’s most important historic sources of liddicoatite.

The tourmaline group is extremely complex. Liddicoatite,  $\text{Ca}(\text{Li}_2\text{Al})\text{Al}_6(\text{Si}_6\text{O}_{18})(\text{BO}_3)_3(\text{OH})_3\text{F}$ , is a calcic lithium-tourmaline end member that was identified as a separate species 25 years ago (Dunn et al., 1977). These authors named the mineral after Richard T. Liddicoat, then president of GIA, in honor of his enormous contributions to gemological knowledge and education. At the time it was only the sixth tourmaline species to be recognized; currently 13 end-member species are known (see Hawthorne and Henry, 1999). Liddicoatite is one of

three *lithium tourmalines* with the general formula  $(\text{Ca}, \text{Na}, \text{K}, \square)(\text{Li}, \text{Al})_3\text{Al}_6\text{Si}_6\text{O}_{18}(\text{BO}_3)_3(\text{OH})_3(\text{OH}, \text{F})$ , which are defined on the basis of their X-site occupancy: Ca = liddicoatite, Na = elbaite, and a vacant ( $\square$ ) X site = rossmanite. Elbaite is the most abundant gem tourmaline, whereas rossmanite has so far been identified from few localities (Johnson and Koivula, 1998b; Selway et al., 1998), and typically is not of gem quality. However, neither can be separated from liddicoatite without quantitative chemical analysis. Therefore, in this article we use the group name *tourmaline* to refer to material that has not been chemically analyzed.

Although liddicoatite is well characterized mineralogically, little has been published about the history, sources, and gemology of this tourmaline species in particular. This article focuses on liddicoatite from Madagascar—which is the principal historic source—and in particular on the Anjanabonoina pegmatite,

---

See end of article for About the Authors and Acknowledgments.  
GEMS & GEMOLOGY, Vol. 38, No. 1, pp. 28–53.  
© 2002 Gemological Institute of America

which has been the most important producer of liddicoatite-elbaite tourmaline from that country. Chemical data for liddicoatite from other world localities (i.e., Brazil, Canada, "Congo," Czech Republic, Mozambique, Nigeria, Russia, Tanzania, and Vietnam) are included in Appendix A.

## HISTORY AND MINING

**Gem Tourmaline in Madagascar.** In the 1500s and 1600s, French explorers reported topaz, amethyst, aquamarine, and other gem minerals from Madagascar (Lacroix, 1913a, Wilson, 1989). However, initial investigations found little gem-quality material, apparently because they focused on river mouths and areas close to the coast. In 1890, a colleague of French scientist A. Grandidier brought a large rubellite crystal from the Mount Ibity area (also spelled Bity; figure 2) south of Antsirabe to the National Museum of Natural History in Paris (Lavila, 1923). By 1893, Grandidier had found colored tourmaline *in situ* at pegmatites in the Betafo region (west of Antsirabe). The first significant pegmatite mining occurred in the early 1900s (Besairie, 1966).

Alfred Lacroix, a professor at the National Museum of Natural History in Paris, provided some of the first descriptions of Madagascar tourmaline and other gem minerals. His comprehensive work on the mineralogy of France and its colonies included descriptions of the crystallography, morphology, and color zoning of tourmalines brought back to France by early colonists (see Lacroix, 1893, 1910). Dabren (1906), a French mining engineer in Madagascar, described several localities for gem tourmalines, including the important pegmatite areas around Antsirabe and Fianarantsoa. A detailed early description of polychrome tourmaline from the "Ankaratra" area was given by Termier (1908). (Note that the Ankaratra massif, which is located about 50 km north of Antsirabe, is a volcanic area that is not a known source of tourmaline; the locality was probably reported in error.) That same year, Lacroix (1908) described gem-tourmaline-bearing pegmatites in the Sahatany Valley area (south of Antsirabe).

In 1910, Lacroix illustrated a slice of polychrome tourmaline from Anjanabonoina as part of his description of the geology, localities, and properties of tourmaline from the Vakinankaratra (Antsirabe), Ambositra, and Fianarantsoa districts. In describing the color zoning, he noted the distinctive star shape made by three red bands intersecting at 120° in

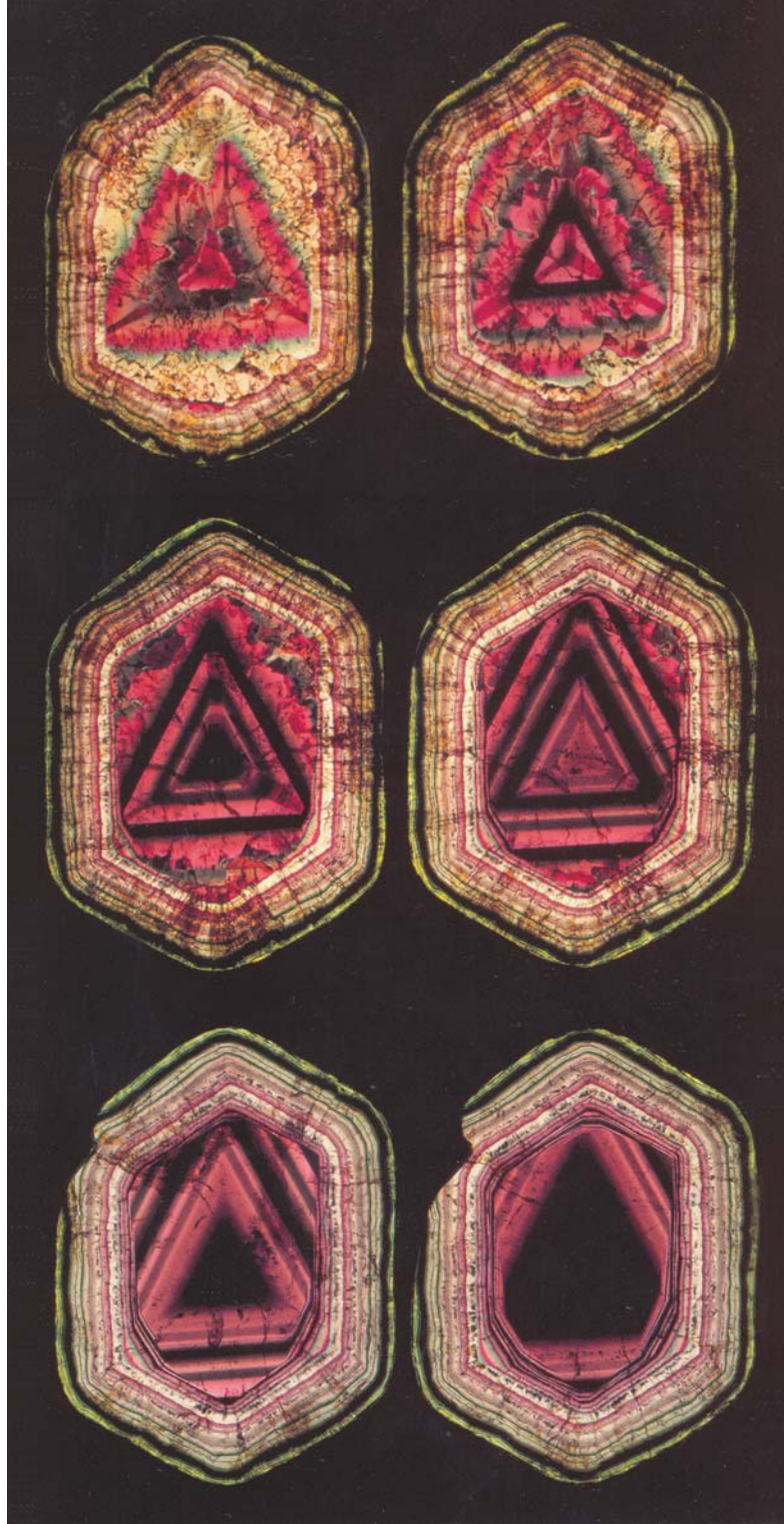


Figure 1. These slices of tourmaline from Anjanabonoina were cut from a single crystal, and show the dramatic progression of color zoning seen perpendicular to the *c*-axis (from top to bottom). The top two slices display a trigonal star pattern and "aggregate type" zoning (see Benesch, 1990). All have an outer region consisting of fine-scale color zoning that is roughly parallel to the prism faces. The slices measure 10 cm in longest dimension and are courtesy of Pala International; composite of photos © Harold and Erica Van Pelt.

some Madagascar tourmaline sections cut perpendicular to the c-axis (see, e.g., figure 3). Physical and chemical data also were included, and two chemical analyses—for a pink crystal from “Maroando” and a red sample from “Antaboka”—correspond to those of tourmalines that later came to be identified as liddicoatite. (Maroandro and Antaboaka, as they are typically spelled today, are located near Tsilaisina and southern Antsirabe, respectively, on opposite ends of the Sahatany Valley.) The data were reprinted from work done by L. Duparc at the University of Geneva (see, e.g., Duparc et al., 1910). Lacroix (1913b) illustrated the diverse morphology shown

Figure 2. The Anjanabonoina mine is located in the central highlands of Madagascar, approximately 55 km west of Antsirabe. This region hosts numerous gem-bearing pegmatites that are famous for producing beautiful tourmaline, morganite, kunzite, and other minerals for over a century.

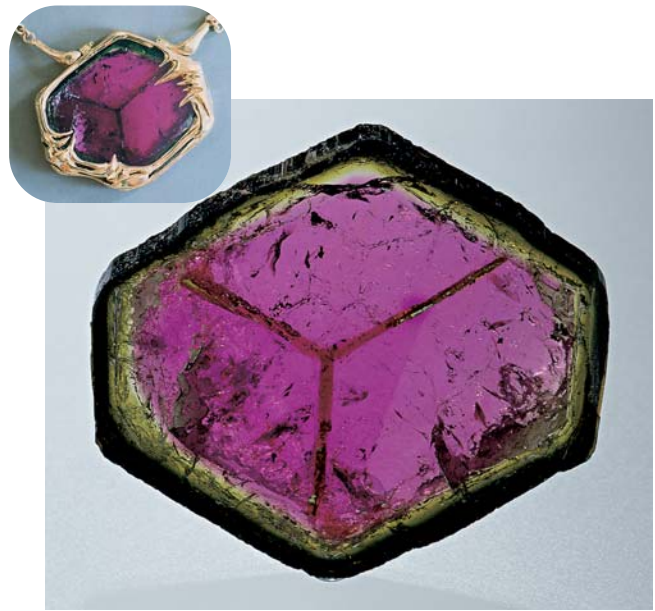


Figure 3. A trigonal star pattern formed by red color bands is evident in the pink portion of this tourmaline slice (5.5 × 4.5 cm) from Anjanabonoina. Courtesy of Allerton Cushman & Co.; photo © Robert Weldon. The inset shows this same slice set in an 18K gold pendant; courtesy of Rodney Blankley, Blankley Gallery, Albuquerque, New Mexico.



by Madagascar tourmaline. While all of this early work is published in French, some of the information has been summarized in articles in English (see Lacroix, 1913a; Gratacap, 1916).

Lacroix undertook the first detailed mineralogical expedition to Madagascar in 1911 (see Lacroix, 1913a), and a decade later he published the classic

Figure 4. Some of the typical crystallographic forms of tourmaline from Anjanabonoina are shown here (after Lacroix, 1922a). The crystals are bounded mainly by the prisms  $a\{11\bar{2}0\}$  and  $m\{10\bar{1}0\}$ ; the rhombohedrons  $r\{10\bar{1}1\}$ ,  $o\{02\bar{2}1\}$ , and  $k\{05\bar{5}1\}$ ; and minor scalenohedrons  $t\{21\bar{3}1\}$ ,  $e\{15\bar{6}2\}$ , and  $n\{24\bar{6}1\}$ .

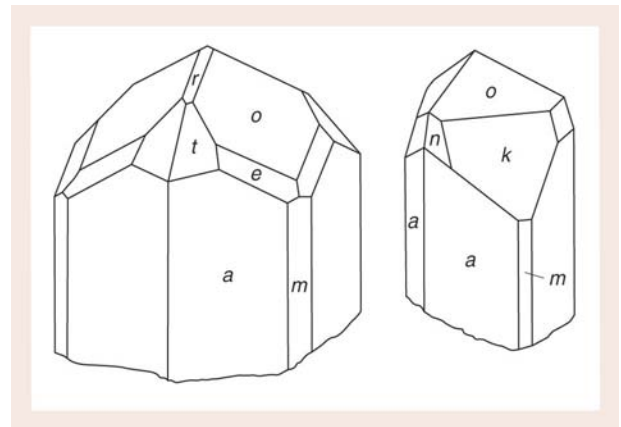


Figure 5. The historic Anjanabonoina mining area is situated on a low hill that contains several pegmatites and associated eluvial deposits. This view of the northeastern side shows a portion of the eluvial workings (right), as well as several white dump piles from pegmatite exploration activities in 1995–1996. The lower dump in the center marks the entrance to a 185-m-long prospect tunnel, and those further up the hill show the location of exploratory shafts (up to 45 m deep). Photo by Federico Pezzotta, January 1996.



three-volume reference work on the minerals of Madagascar (Lacroix, 1922a,b, 1923). In the first volume, he reported that the original tourmaline deposits were depleted, and that Anjanabonoina was the only deposit being mined for tourmaline. He illustrated the common crystallographic forms of this tourmaline (figure 4; see also Goldschmidt, 1923), and noted that particularly large and beautiful crystals were found in the eluvial workings there. Detailed descriptions of the color zoning and corresponding physical properties in Madagascar tourmaline (including crystals from Anjanabonoina) also were provided. Chemical analyses in this report revealed the relatively calcium-rich composition of Anjanabonoina tourmalines.

Several decades passed before the next important mineralogical work on Madagascar tourmaline was published, by Besairie (1966). Not only did this work mention the colored tourmalines and associated minerals found at Anjanabonoina and other pegmatites in central Madagascar, but it also included detailed locality maps. Later, from his 1976 visit, Strunz (1979) described the situation at the Anjanabonoina mine, and in 1989 W. E. Wilson provided a detailed account of the mineralogy. More recently, the color zoning of Madagascar tourmaline has been beautifully depicted (see, e.g., Benesch, 1990; Wöhrmann, 1994; Zang, 1996).

**The Anjanabonoina Deposit.** The Anjanabonoina mining area (figure 5) reportedly was discovered in 1894 by Emile Gautier (Bariand and Poirot, 1992). Léon Krafft began intensive mining in the early 1900s. The greatest activity occurred between 1920

and 1925, with 80 workers on site (Guigues, 1954). Large quantities of multicolored tourmaline and exceptional morganite were recovered (Wilson, 1989). By the time operations ceased in 1930, miners had explored only the eluvial portion of the deposit along the eastern slope of the hill (figure 5). (For mining methods used at the time to recover gems in Madagascar, see Lacroix [1922a] and Besairie [1966].) Very limited surface digging by local miners continued until the 1960s.

In 1965, Eckehard Petsch of the Julius Petsch Jr. Company (Idar-Oberstein, Germany) traveled to Madagascar and learned about the unusual color-zoned tourmalines from Anjanabonoina. With the assistance of Madame Liandrat of Antananarivo (Krafft's daughter), Mr. Petsch visited the mining area in 1967, after an arduous trip that involved nearly two days of walking. He found tourmaline crystals in the dumps of the abandoned mine and determined that a significant portion of the deposit still had not been mined (Bancroft, 1984).

Mr. Petsch's Madagascar company, Société Germaadco, acquired the Anjanabonoina deposit in 1970. This venture established roads, built housing and a school for the miners and their families, and began mining tourmaline in 1972 from the dumps and eluvial deposits downslope of the pegmatites. By 1974 there were more than 100 workers on site (Bariand and Poirot, 1992), and the mine was mapped in detail. Further mining of the pegmatites themselves took place in the upper-middle portion of the hill (figure 6). Some of the tunnels driven at this time reached up to 100–200 m long. He operated the mine until 1979, when the government of

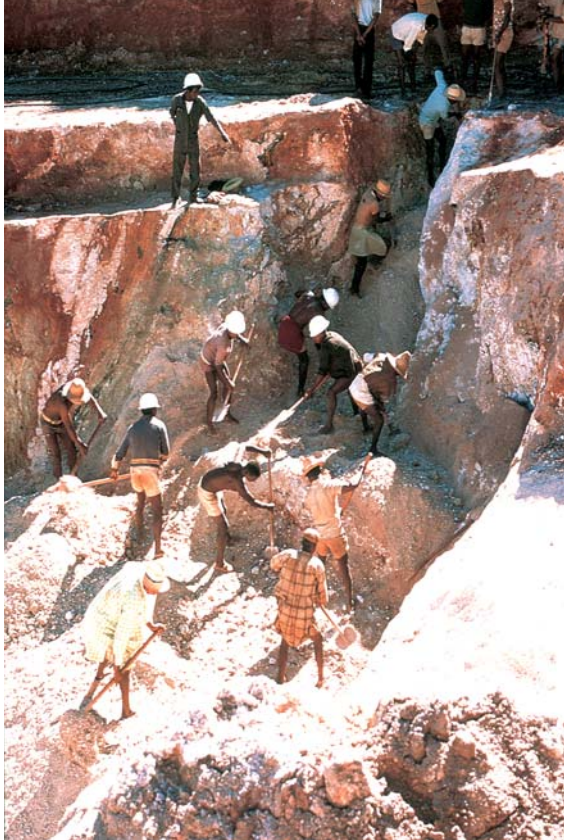


Figure 6. Miners excavate one of the pegmatites at the Anjanabonoina deposit for Société Germa dco in 1975. Photo by Eckehard Petsch.

Madagascar imposed a new law that required the transfer of ownership of all foreign mining companies to Malagasy nationals. Société Germa dco was placed under the control of a Malagasy engineer, Randrianariso lo Benjamin (a previous employee of E. Petsch), together with a Bulgarian partner.

The new owners focused on mining the large pegmatite dikes still in place, as well as tunneling to explore the potential of the deposit at depth. In addition, they dug an open pit 1.6 km southwest of the historic mine to investigate some large pegmatite veins that probably form a continuation of the Anjanabonoina pegmatites. Although this pit was unproductive, in 1984 a large tourmaline pocket was discovered on the western slope of the hill, near the original mining village. Crystals from this pocket were exported by the Bulgarian partner, but he was forced to leave Madagascar shortly thereafter due to problems with Société Germa dco and the local people. Société Germa dco remained the legal owner of the claims, but lost control of the mine when hundreds of people, excited by the discovery, began digging there illegally.

Locals continued to work the area manually for many years, resulting in hundreds of dangerous pits up to 40 m deep. The roads and structures built during past mining activities were destroyed by erosion

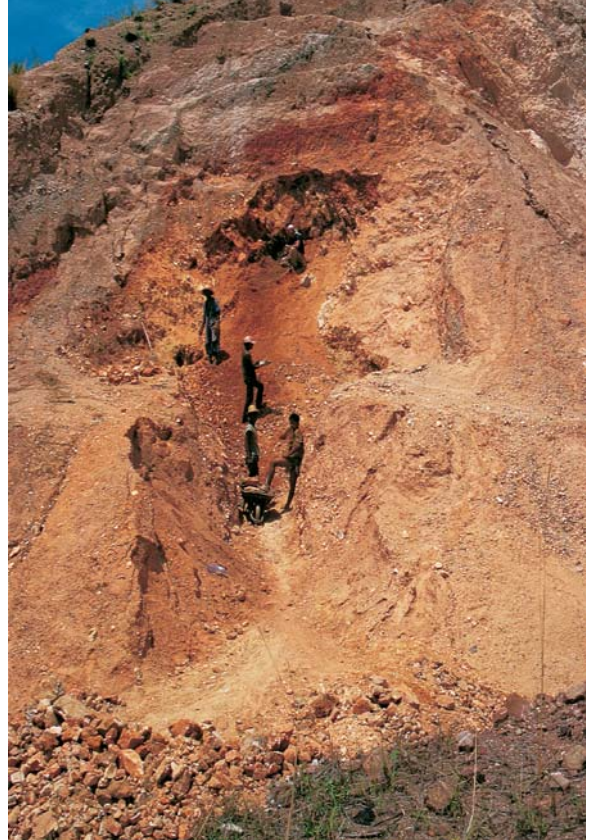


Figure 7. Relatively recently, the Anjanabonoina deposit was explored by Fretosoa Co. Here, deeply weathered pegmatite is mined from the upper-eastern part of the deposit (Sarodivotra workings, December 1995). This area produced significant crystals of dravite and liddicoatite. Photo by Federico Pezzotta.

during the rainy seasons, making it necessary for the miners to transport their gems on foot to be sold in the villages of Ambohimambola and Betafo. In 1991, the discovery of another large pocket led to a new period of unrest in which several miners were killed. When no significant new discoveries were made during the next few years, many of the miners abandoned the locality.

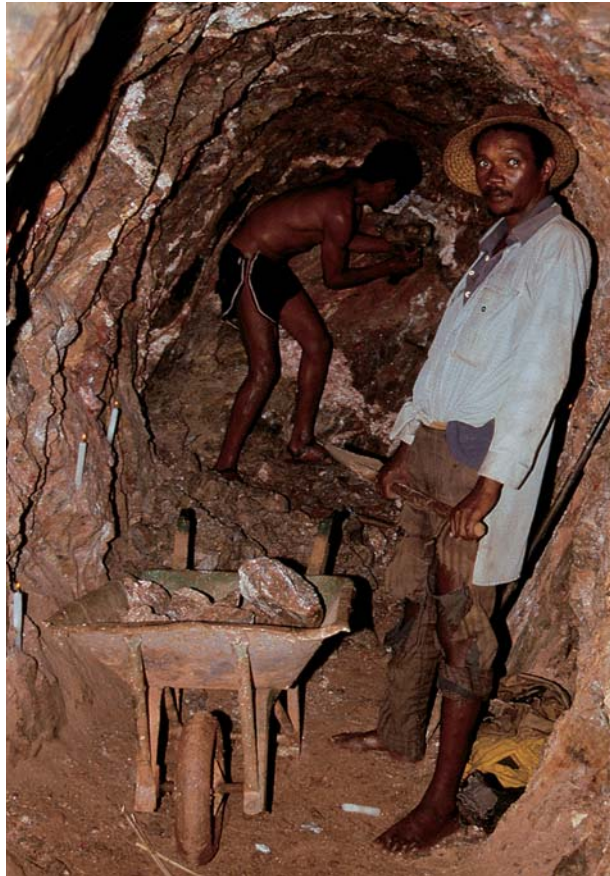
In 1995, one of the authors (FP) led Fretosoa Company, an Italian-Malagasy joint venture, in evaluating the gem potential of the central highlands. After visiting Anjanabonoina, he contacted Germa dco's Benjamin and a partnership between Germa dco and Fretosoa was formed. In the next two years, they developed a series of surface and underground workings (figures 7 and 8), which included four shafts that were 45–55 m deep and a 185-m-long subhorizontal tunnel that reached the pegmatite core zone. From these workings, FP collected enough geologic and structural data to create a three-dimensional model of the deposit and recognize that a significant portion of the gem-bearing core zone was still unmined. However, activity halted following the 1997 deaths of Mr. Benjamin

(who was also mine engineer) and Fretosoa chief Guisepe Tosco. With the mine no longer under strict control, the equipment owned by Fretosoa Co. was subsequently stolen, and the tunnels and pits collapsed or were destroyed by the activities of local miners. Currently, the mine is nearly abandoned, with only a few locals digging on the surface during the rainy season, when there is water available for washing the mined material (figure 9).

### LOCATION AND ACCESS

The Anjanabonoina mine is located about 55 km west-southwest of Antsirabe in the Antananarivo

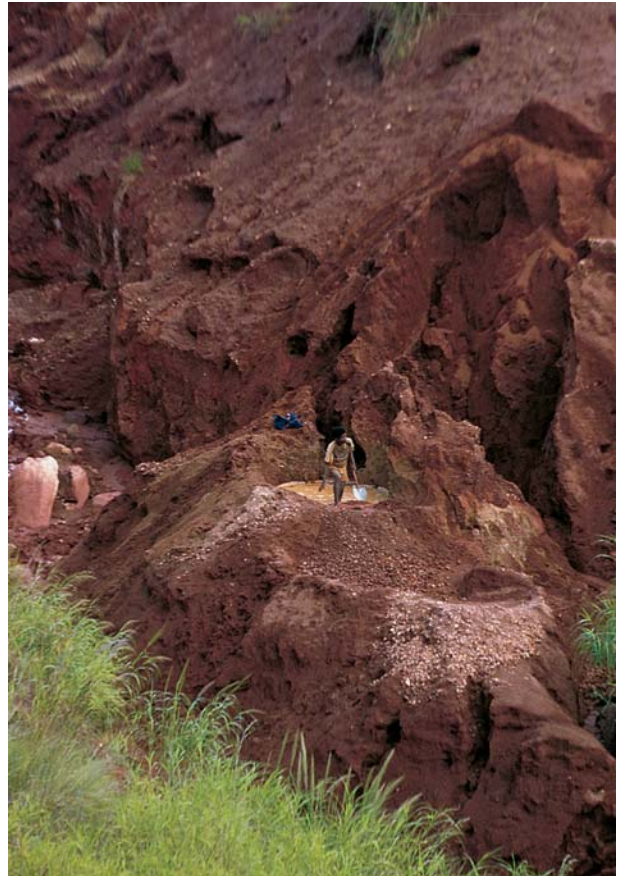
*Figure 8. An exploration tunnel was dug by hand from the northeastern side of the Anjanabonoina deposit by Fretosoa Co. during October 1995 to December 1996. Shown here at 160 m from the surface, small kaolinized pegmatite veins can be seen crosscutting the weathered quartzite. Note the candles on the left that were used for illumination. Photo by Federico Pezzotta.*



Province of central Madagascar (again, see figure 2). The deposit is situated on a hill (1,400 m elevation) at 19°55' S and 46°32' E, 2.5 km east of Ikaka Mountain (1,781 m). From Antsirabe, a national highway leads 56 km to the intersection with the paved road that proceeds 10 km southwest to the village of Ambohimambola. From there, a track originally graded by Société Germaadco in the early 1970s continues south-southwest for about 32 km, crossing the Ipongy River to the mine. Today, this track is impassable by vehicle, so access to the mine is possible only by foot. The journey from Antsirabe takes about two days, with the trip feasible only during the dry season, from late April until the beginning of November.

The authors do not recommend traveling to the Anjanabonoina area. Because of potential security problems, any foreigner who wishes to visit the

*Figure 9. In recent years, the surface deposits at Anjanabonoina have been worked by local people, who use pools of rainwater to wash the material. Photo by Federico Pezzotta.*



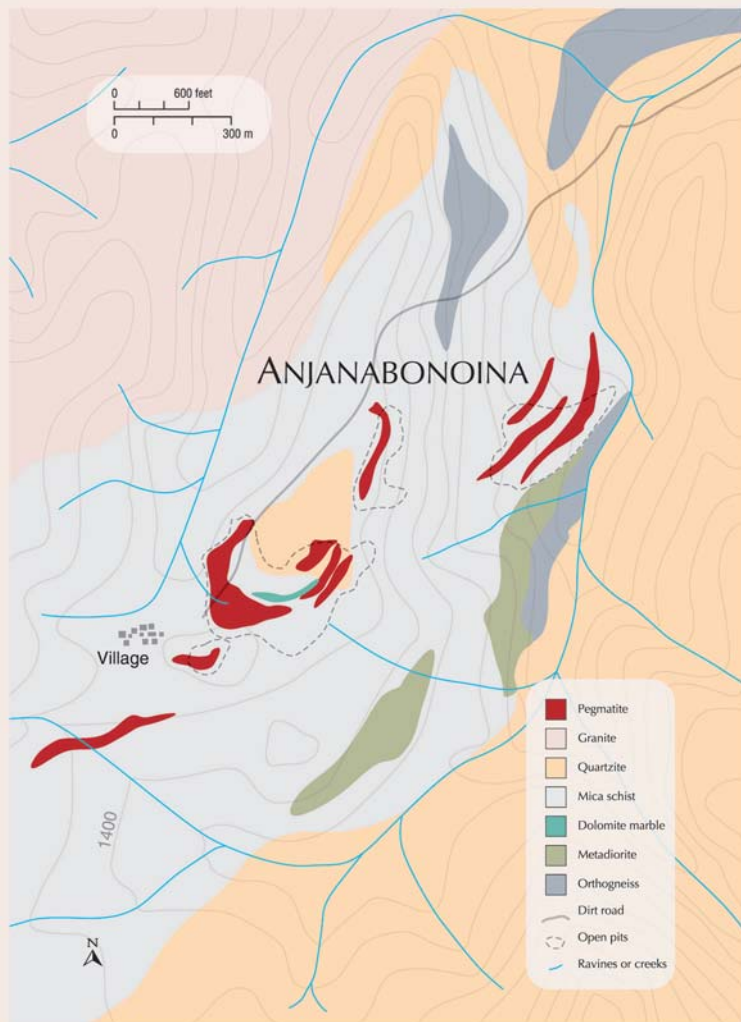


Figure 10. This generalized geologic sketch map of the Anjanabonoina deposit shows a series of south-southwest-trending pegmatites that have intruded schist, quartzite, and marble of the Itremo Group. The main eluvial deposits are located on the southern side of the hill near the village. Map by Federico Pezzotta.

region must first inform the local police. Note, too, that travelers to this area are at risk for malaria, especially during the rainy season.

## GEOLOGY

**Regional Geology.** The western part of Madagascar consists mostly of Mesozoic sedimentary rocks, whereas the central and eastern portions consist mainly of Proterozoic metamorphic and igneous basement rocks (see, e.g., Ashwal and Tucker, 1999). The crystalline basement is part of the Mozambique orogenic belt (or East African Orogen), which originally extended through eastern Africa and Madagascar, Sri Lanka, India, and East Antarctica when they were still part of the Gondwana supercontinent (see, e.g., Petters, 1991). A large vari-

ety of gem deposits are associated with the Mozambique Belt (see Malisa and Muhongo, 1990; Menon and Santosh, 1995; Dissanayake and Chandrajith, 1999; Milisenda, 2000). The rocks in this belt underwent extensive metamorphism, plutonism, folding, and faulting during the latter part of the Pan-African orogeny, which occurred over an extended period from at least 950 to about 450 million years (My) ago (see, e.g., Petters, 1991). The last magmatic cycle of the Pan-African event occurred from about 570 to 455 My (Paquette and Nédélec, 1998; Fernandez et al., 2001), and generated granitic plutons and associated pegmatite fields (Zhdanov, 1996; Pezzotta, 2001). The gem-bearing pegmatites are undeformed by large-scale tectonic processes, and are thought to have formed in the later part of this cycle (i.e., younger than 490 My—Giraud, 1957; Fernandez et al., 2000).

Many of the gem-bearing pegmatites in central Madagascar, including Anjanabonoina and the famous localities in the Sahatany Valley, are hosted by rocks of the Itremo Group, in a tectonic unit known as the Itremo thrust sheet (see, e.g., Collins, 2000). The Itremo Group is characterized by a lower unit of gneiss and an upper unit of quartzites, schists, and marbles (see Fernandez et al., 2001). Both units are locally intruded by the pegmatites, which probably formed via fractional crystallization

Figure 11. Extensive hydrothermal alteration of the host rock occurred adjacent to the Anjanabonoina pegmatites. The calcium needed to form liddicoatite was probably derived from the metasedimentary host rocks. Here, the contact between a pegmatite (top right) and marble (bottom left) is shown. Black tourmaline veins can be seen along the contact and penetrating into the marble. Photo by Federico Pezzotta.



of granitic plutons emplaced at relatively shallow depths (Pezzotta and Franchi, 1997).

**Geology of the Anjanabonoina Area.** Laplaine (1951) described the general geology of the Anjanabonoina region. The pegmatites composing the historic part of the mining area are exposed over an area measuring 800 × 300 m (figure 10). These dikes form part of a larger aplite-pegmatite system that extends south-southwest of the Anjanabonoina area for about 2 km. (Aplite is a light-colored igneous rock characterized by a fine-grained texture composed primarily of quartz, potassium feldspar, and sodic plagioclase; Jackson, 1997.) For simplicity, the dikes will be referred to simply as pegmatites here. The major pegmatites dip gently north-northwest and range from 2 to 12 m thick.

The pegmatites were emplaced in a complex geologic environment, probably at the contact between the lower and upper units of the Itremo Group. The host rocks consist of quartzites, schists, and marbles that are locally tourmalinized near the pegmatites (figure 11). Large areas of the pegmatites are deeply kaolinized by the activity of late-stage hydrothermal fluids (De Vito, 2002). The rocks are also deeply weathered—to depths exceeding 20 m—particularly in the southern portion of the mining area where extensive eluvial deposits were worked.

Lacroix (1922b) classified the Anjanabonoina pegmatites as “sodalithic” (i.e., sodium- and lithium-rich). According to the modern classification of pegmatites proposed by Černý (1991), the Anjanabonoina pegmatites have mineralogical characteristics intermediate between the LCT (lithium, cesium, and tantalum) and NYF (niobium, yttrium, and fluorine) families of the Rare-Element and Mirolitic classes (Pezzotta, 2001).

Gem-bearing “pockets” or cavities are rather rare in these pegmatites, but they may be very large (i.e., several meters in maximum dimension). The pockets are surrounded by kaolin clay and contain assemblages of quartz, microcline feldspar (amazonite), albite feldspar (cleavelandite), dravite-elbaite-liddicoatite tourmaline, spodumene (kunzite), native bismuth, spessartine, beryl (morganite), hambergite, danburite, phenakite, and scapolite (Pezzotta, 1996; De Vito, 2002). The tourmaline crystals are large (typically weighing up to 20 kg each; see, e.g., figure 12), and most have a black outer “skin” (E. J. Petsch, pers. comm., 2002). The largest tourmaline crystal recovered by Mr. Petsch measured 80 cm tall and 32 cm in diameter.



Figure 12. Tourmaline crystals from Anjanabonoina are typically large. This doubly terminated liddicoatite crystal weighs 17.8 kg, and measures 33 cm tall and 22 cm wide. Although the crystal appears dark, if sliced it would probably yield spectacular slabs. Courtesy of Eckehard Petsch; photo by R. Appiani.

Benesch (1990—figure 36) depicted the base of a 40-cm-diameter crystal from Anjanabonoina.

## PRODUCTION AND DISTRIBUTION

By 1912, the total production of colored tourmaline from Anjanabonoina was 1,675 kg (Guigues, 1954). According to Bariand and Poirot (1992), production decreased in the next 10 years, yielding a total of about 15 kg of rubellite and multicolored tourmaline. But between 1920 and 1925 the tourmaline output increased dramatically, with almost 1,700 kg mined. Production was negligible from 1950 to 1970. E. J. Petsch (pers. comm., 2002) recalled that Société Germadco recovered several thousand kilograms of red and polychrome tourmaline in the 1970s. During the 1980s and early 1990s, some tonnes of gem tourmaline were recovered, but no specific data are available. More recently, there has been small, sporadic production from local miners working with hand tools (E. J. Petsch, pers. comm., 2002).

According to statements to one of the authors (FP) from older miners and Malagasy gem and mineral dealers in Betafo and Antsirabe, major pockets were discovered at Anjanabonoina in 1972, 1978, 1984, and 1991. The 1978 pocket was probably the largest, with 2.6 tonnes of polychrome and red tourmaline crystals weighing up to 20 kg each (see



Figure 13. This duck is carved from Madagascar tourmaline and is mounted on a rutilated quartz bowl. The body, wings, and tail are carved from separate pieces. Courtesy of Herbert Klein, Idar-Oberstein; photo © Harold & Erica Van Pelt.

Pezzotta, 2001). The 1984 pocket produced about 2 tonnes of similar tourmaline, as well as several other gem materials (see Wilson, 1984). The quantity of tourmaline from the 1991 pocket is not known, although FP was told of a single sale of 600 kg of red tourmaline from this find.

Lacroix (1922a,b) reported that, besides the well-known polychrome variety, gem tourmaline from Anjanabonoina occurred in many homogeneous colors: red to violetish red (with faceted stones approaching 40 ct) grading into pink, “yellowish pink,” or colorless; “amethyst” violet to colorless; various greens, browns, and yellows; and pale blue. Facetable morganite, kunzite, spessartine, and danburite also were produced.

In the early part of the 20th century, the gem material from Anjanabonoina went first to France and later also to Germany and Switzerland (Pezzotta, 2001). Lacroix (1922b) noted that after cutting, the best-quality gems (which presumably included tourmaline) were commonly sold as Brazilian goods. During the early 1970s, the majority of the tourmalines produced by Société Gemadco were exported

to the Julius Petsch Jr. Company in Idar-Oberstein (E. J. Petsch, pers. comm., 2002).

### PROCESSING: SLICING AND CARVING

Lacroix (1908) and Termier (1908) first illustrated the triangular polychromatic zoning in Madagascar tourmaline (see also Wöhrmann, 1994). To reveal the beautiful zoning, most multicolored liddicoatite is fashioned as polished slices (see figure 1 and Benesch, 1990). Liddicoatite provides gem artists with a wide variety of colors and patterns, and so has been used to great advantage in carvings (figure 13) and intaglios (figure 14). More recently, partially faceted stones have gained popularity (Johnson and Koivula, 1998a; Weldon, 2000).

Gerhard Becker, who purchased much of the tourmaline from the Julius Petsch Jr. Company, reportedly first commercialized the cutting of liddicoatite into slices to display the color zoning patterns more dramatically (E. J. Petsch, pers. comm.,

Figure 14. Tourmaline from Alakamisy Itenina, Madagascar, was used in this intaglio, which was designed and carved by Ute Bernhardt with permission from Mikhail Baryshnikov to depict his representation of an older man in the ballet Heart Beat. Note the “aggregate-type” color zoning. Photo © GIA and Tino Hammid.

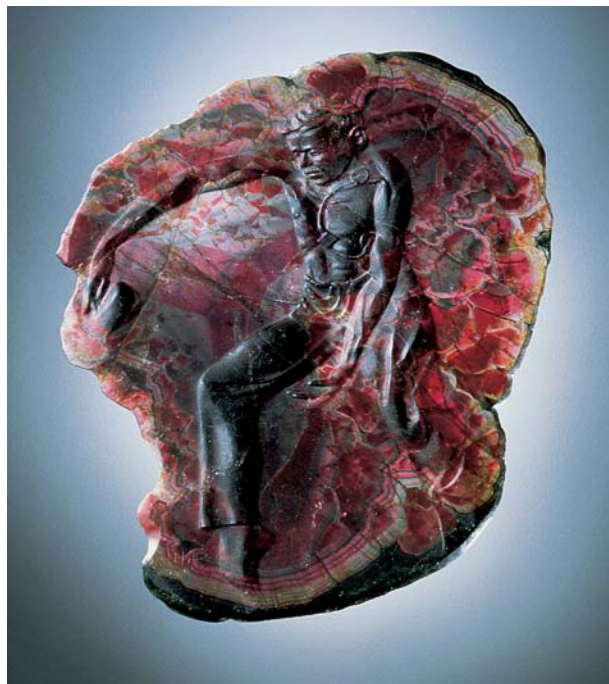




Figure 15. These study samples illustrate the color diversity found in Madagascar tourmaline. The six slices on the left (1.9 to 7.0 cm) were represented as being from Anjanabonoina; microprobe analysis of one (pink and light green, to the lower right) revealed that it was liddicoatite. The two slices on the right (3.0 and 4.4 cm) also were liddicoatite, except for two elbaite analyses in the green rim of the larger slice. Left—Courtesy of William Larson, right—courtesy of Richard T. Liddicoat (top) and GIA (bottom); photos by Maha Tannous.

2002). He described the slicing of one such tourmaline in a 1971 article tantalizingly titled “70 pound tourmaline crystal produces multicolored slabs.” GIA’s Richard T. Liddicoat happened to visit Becker’s shop shortly after he sliced the crystal, and photographed the progression of patterns that were revealed from its base toward the termination (see Becker, 1971). Because of their large size, Madagascar tourmaline slices also have industrial applications: Since World War II, they have been used for radio oscillator plates and pressure gauges (Fron del, 1946; Althaus and Glas, 1994).

## MATERIALS AND METHODS

We studied a total of 27 samples of Madagascar tourmaline (figures 15–17). These included eight polished multicolored slices (figure 15), six of which have a probable provenance of Anjanabonoina (W.

Larson, pers. comm., 2001) with the other two from unspecified localities in Madagascar. All of the slices were cut perpendicular to the c-axis; they ranged from  $1.5 \times 1.9$  cm to  $5.0 \times 7.0$  cm. We also examined nine faceted (1.17–12.88 ct) and two freeform (1.24–1.29 ct) parti-colored samples that were purchased in Antsirabe, again with a probable Anjanabonoina provenance (T. Cushman, pers. comm., 2002; see figure 16). As a third group, we looked at five faceted purplish red tourmalines (1.05–6.20 ct) from Anjanabonoina that were originally obtained by A. Lacroix in the early 20th century and three faceted purplish red tourmalines (2.98–5.48 ct) from Anjanabonoina purchased by GIA from E. Petsch in 1981 (figure 17). These last three stones were analyzed by electron microprobe (two spots per sample) in 1982 at the California Institute of Technology in Pasadena, California, and confirmed as liddicoatite.

Figure 16. Parti-colored tourmaline from Madagascar is fashioned into dramatic step cuts and freeform polished stones, as shown in these study samples (1.17–3.56 ct on the left, and 4.00–12.88 ct on the right), which are probably from Anjanabonoina. Despite the similarities in their appearance, electron-microprobe data from the samples in the left photo revealed that two were elbaite, three were liddicoatite, and three contained zones of both species (e.g., the kite-shaped stone on the bottom right). Courtesy of Allerton Cushman & Co.; photos by Maha Tannous.





Figure 17. A range of tone and saturation is shown by these purplish red liddicoatites (1.05–6.20 ct) from Anjanabonoina. Courtesy of the National Museum of Natural History in Paris and the GIA collection (i.e., the stones on the far left and right, and the oval in the center); photo by Maha Tannous.

Standard gemological properties were obtained on all samples, to the extent possible. A GIA GEM Instruments Duplex II refractometer with a near-sodium-equivalent light source was used for refractive index readings. Specific gravity was determined by the hydrostatic method, although four of the slices could not be measured because they were too large for our immersion container. Reaction to ultraviolet radiation was viewed in a darkened room with four-watt long- and short-wave UV lamps. Because the absorption spectra for tourmalines typically do not provide much meaningful information (see, e.g., Webster, 1994), we did not perform spectroscopy on these samples. Internal features were observed with a standard gemological microscope, and a polariscope was used to view strain. Laser Raman microspectrometry, performed with a Renishaw 2000 Ramascope at GIA in Carlsbad, was used to identify mineral inclusions in several samples.

Quantitative chemical analyses were obtained by electron microprobe at the University of New Orleans, Louisiana (ARL-SEM-Q instrument), and at the University of Manitoba, Canada (Cameca SX 50 instrument). Most of the Madagascar study samples were analyzed: three slices, two freeforms (each of which had a large flat area), and 14 faceted stones. In addition, a small fragment from the tourmaline crystal that is illustrated in Appendix A was analyzed by electron microprobe. As part of an ongoing project by one of the authors (WS) to characterize

the composition of gem tourmaline, chemical data were also obtained for several samples from other localities that are known or suspected to produce liddicoatite: two faceted ovals (3.95 and 20.47 ct; the latter stone was described by Koivula and Kammerling [1990]), reportedly from Minas Gerais,

**TABLE 1.** Properties of liddicoatite-elbaite from Madagascar.

Property	Description
Color	Diverse color range, commonly in complex zones and patterns, arranged predominantly parallel to pyramidal faces. Homogeneous colors include red to violetish red (most common), grading into pink, pinkish yellow, and colorless; "amethyst" violet to colorless; various greens and browns; pale blue; and yellow of various hues. <sup>a</sup>
Pleochroism	Weak to strong, depending on color
Clarity	Transparent to translucent; an opaque black skin is present on most crystals
Morphology	Stout prismatic crystals with trigonal symmetry, bounded by faces of the prism, rhombohedron, and scalenohedron; striated parallel to the c-axis <sup>a</sup>
Optic character	Uniaxial negative (may contain biaxial zones); strain commonly observed with polariscope
Refractive indices	
$n_{\omega}$	1.635–1.651 (1.637±0.003 <sup>b</sup> )
$n_{\epsilon}$	1.619–1.634 (1.621±0.003 <sup>b</sup> )
Birefringence	0.014–0.027 (0.019 <sup>b</sup> )
Specific gravity	3.05–3.07 for parti-colored stones and slices; 3.06–3.11 for purplish red samples (3.052–3.092 <sup>a</sup> , 3.00–3.07 <sup>b</sup> )
Dispersion	0.017 (B to G) <sup>c</sup>
Hardness	7–7½ <sup>b</sup>
Luster	Vitreous on fracture surfaces <sup>d</sup>
Cleavage	Poor on {0001} or absent <sup>d</sup>
UV fluorescence	
Short-wave	Inert to moderate greenish yellow to golden yellow
Long-wave	Inert
Internal features	Color zoning, accompanied by growth zoning in some samples; strain patterns; interconnected network of wavy, partially healed fractures that are composed of stringers, minute lint-like particles, and irregular forms (both one- and two-phase liquid-gas), commonly with a wispy appearance; feathers; needle-like tubes; pinpoints; albite, tourmaline, xenotime, and quartz inclusions; negative crystals and cavities

Properties were obtained in this study unless otherwise noted:

<sup>a</sup>Lacroix (1922a)

<sup>b</sup>Dunn et al. (1978)

<sup>c</sup>Webster (1994)

<sup>d</sup>Dunn et al. (1977)

Brazil; one polished slice from Vietnam; one polished crystal (from Abuja) and six polished slabs from unspecified localities in Nigeria; five polished slabs from "Congo"; and a small crystal fragment from Chita, eastern Transbaikalia, Russia. From four to 14 spots per stone were analyzed.

Since some elements in tourmaline (i.e., boron, lithium, and hydrogen) cannot be measured by electron microprobe, a series of assumptions must be made when calculating the cations in the formulas. For consistency, we calculated the cations for all of the analyses—whether obtained by us or from the literature—according to standard conventions (see Deer et al., 1992). Contents of  $\text{Li}_2\text{O}$ ,  $\text{B}_2\text{O}_3$ , and  $\text{H}_2\text{O}$  also were calculated, except for those analyses for which Li, B, and H were determined by analytical means.

## RESULTS

Our results confirmed earlier statements in the literature (see, e.g., Webster, 1994) to the effect that liddicoatite and elbaite cannot be separated conclusively without chemical analysis. Both tourmaline species were found in the Madagascar study samples. Although all of the parti-colored tourmalines were represented as liddicoatite, two of the nine samples analyzed by microprobe were elbaite, three were liddicoatite, and three contained both species depending on the particular spot analyzed. All three of the slices analyzed were liddicoatite, but one contained elbaite near the rim. All eight of the purplish red gemstones were liddicoatite. Regardless of the species, the samples showed overlapping properties and therefore the results obtained for liddicoatite and elbaite are not differentiated below or in table 1.

**Visual Appearance and Gemological Properties.** The parti-colored samples displayed multiple closely spaced color zones with sharp to diffuse boundaries, as described by Mitchell (1984). The color zones were commonly arranged in straight, subparallel layers, although some samples had bent or swirled patterns (figures 18 and 19). The colors ranged from pink to purplish red, orangy pink to pinkish orange, yellowish green to bluish green, brownish green to brown to brownish yellow, greenish blue, black, and colorless. Most of these hues were present in a wide range of tones (i.e., light to dark) and saturations (i.e., pale to intense), resulting in considerable variations (see figures 16, 18–19).

The polished slices also showed distinct patterns of color zoning, the two most common of which



Figure 18. Oscillatory (narrow, repeating) zoning is shown by this parti-colored tourmaline that is probably from Anjanabonoina. Note the gradation in pink color intensity within each color zone, and the sharp boundaries with the green layers. Photomicrograph by John I. Koivula; magnified 10 $\times$ .

were triangular zones around the core and concentric layers near the rim. The triangular zones are defined by straight, planar boundaries that are parallel to a pyramidal direction (i.e., a rhombohedron). In some slices, however, the boundary with the central triangle is parallel to the prism faces (i.e., the c-axis). The concentric outer zones are oriented parallel to the prism faces and are typically very narrow.

All samples (other than the slices, which were viewed parallel to the c-axis) showed moderate to strong dichroism in the darker, more saturated colors, and weak pleochroism in the lighter, less saturated areas.

The samples ranged from transparent to translucent, except for zones or layers that were black (opaque). The diaphaneity of the lighter colors was commonly reduced by the presence of abundant inclusions.

When viewed with the polariscope, most of the multicolored samples exhibited birefringence

Figure 19. Color zones in Madagascar tourmaline can display myriad shapes. Strong growth structures are also visible in this sample as a series of straight lines. Photomicrograph by John I. Koivula; magnified 5 $\times$ .





Figure 20. These images show strain patterns in a slice of liddicoatite from Madagascar cut perpendicular to the c-axis. The left view shows the color zoning, whereas the center and right photos were taken with cross-polarized light to show the anomalous birefringence; the image on the right was taken with a first-order red compensator. Although not one of the study samples, it has been confirmed as liddicoatite by electron microprobe analysis (J. Koivula, pers. comm., 2002). Photomicrographs by John I. Koivula; magnified 20×

(strain) patterns. These mottled, lamellar, cross-hatched, and irregular patterns varied in intensity from subtle to distinct. Lamellar birefringence was seen in the outer areas of the slices that showed multiple concentric color zones, but in some samples a patchy appearance was seen in the core, starting at the boundary with the triangular color zones. No strain features were visible in the three homogeneous purplish red samples, except when oriented parallel to the c-axis.

The measurement of refractive indices was problematic for most of the multicolored samples due to significant R.I. variations across the color zones. These zones were generally too narrow to permit accurate R.I. readings of individual color bands, so the shadow cutoff moved according to the viewer's eye position. In such cases the best "average" readings for the upper and lower R.I. values were recorded. Unzoned portions that were large enough to measure independently (found in a few slices and polished stones) yielded sharp R.I. readings. Although

there appeared to be no systematic differences in R.I. or birefringence according to color in these stones, in general they did show significant R.I. variations from one color zone to another (typically  $\pm 0.004$ – $0.007$ ). The maximum variation seen in a single sample was  $n_o = 1.639$ – $1.650$  and  $n_e = 1.620$ – $1.629$ . The range of R.I. values measured in all of the samples was  $n_o = 1.635$ – $1.651$  and  $n_e = 1.619$ – $1.634$ . All of the slabs yielded two R.I. values (parallel to the c-axis) that differed by as much as 0.027. Overall, birefringence varied widely (0.014–0.027), but most values ranged from 0.015 to 0.021.

Specific gravity showed less variation than R.I. The 15 multicolored samples that could be measured with our apparatus had a fairly even distribution of values, ranging from 3.05 to 3.07. The eight purplish red samples had S.G. values of 3.06–3.11.

All of the samples were inert to long-wave UV radiation, and approximately two-thirds were inert to short-wave UV. The 10 (multicolored) samples that fluoresced to short-wave UV showed greenish

Figure 21. Partially healed fractures were ubiquitous in the tourmaline samples. They were typically composed of wavy, intersecting networks of fluid inclusions. Photomicrograph by John I. Koivula; magnified 40×

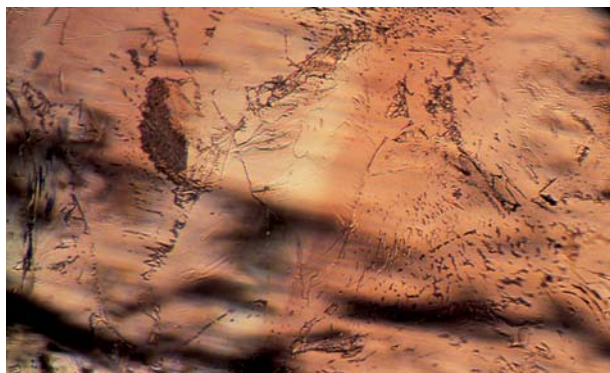
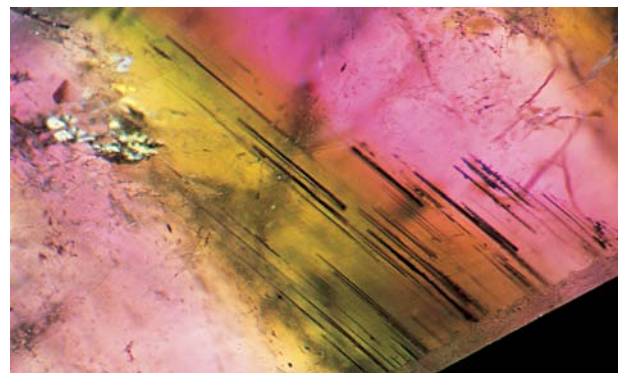


Figure 22. Many of the tourmaline samples contained needle-like tubes that were isolated or arranged in parallel arrays. They were most commonly located within green color zones. Photomicrograph by John I. Koivula; magnified 20×



yellow to “golden” yellow luminescence, of weak to moderate intensity, in specific areas corresponding to certain color zones. Most commonly, these zones were pale pink to colorless, although green, brown, and brownish green or yellow zones also fluoresced in some samples. No phosphorescence was seen.

**Internal Features.** When examined with the microscope, the most obvious internal feature in the multicolored samples was the pronounced color zoning, as described above. In some samples, repeating sequences of color zones had sharp boundaries between one another, and showed gradations in color within each sequence (figure 18). Growth structures were evident in a few samples, mainly along color boundaries and parallel to them; less commonly, crosscutting growth patterns were seen (figure 19).

The strain patterns observed with the polariscope in the multicolored samples were also visible with the microscope in cross-polarized light (see, e.g., figure 20); the same patterns described above were noted. The homogeneous purplish red samples showed no signs of strain except when viewed down the optic axis, revealing subtle wavy or mottled patterns.

Present in all samples were partially healed fractures containing fluid- and/or two-phase (liquid-gas) inclusions (figure 21). These commonly formed wavy, intersecting networks composed of elongate stringers, minute capillaries with a thread- or lint-like appearance (i.e., trichites), or a variety of irregularly shaped forms. Angular cavities were present along partially healed fractures in some samples. Small fractures (“feathers”) also were common. Within the slices, some of the surface-reaching feathers were filled with an opaque white substance that was tentatively identified by Raman analysis as wax or oil.

Other common inclusions were needle-like tubes that were isolated or arranged in parallel arrays. Seen in five samples, these were most commonly located within green color zones (figure 22), and in two samples they appeared to start at minute colorless mineral inclusions showing high relief. Many other mineral inclusions were noted. In eight samples, rounded, colorless crystals formed isolated inclusions and (less commonly) groups; in five of the samples, these were identified by Raman analysis as albite (see, e.g., figure 23). Colorless to pale green crystals with low relief, seen in two parti-colored liddicoatite samples, were identified by Raman analysis as tourmaline; they varied from stubby to prismatic (figure 24).

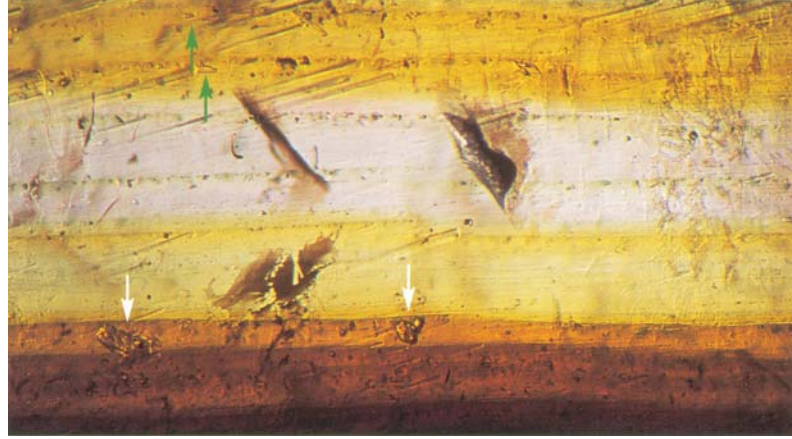
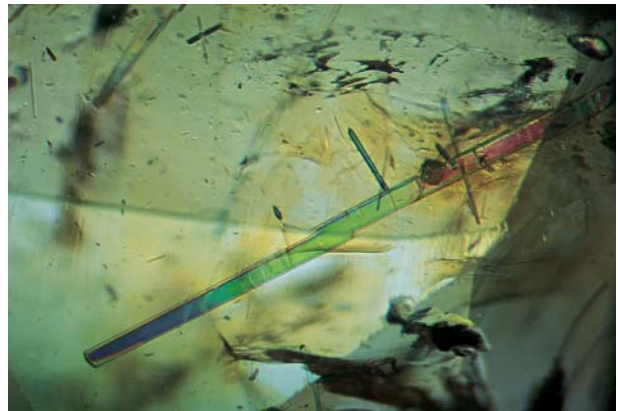


Figure 23. A light brown zone in this parti-colored elbaite-liddicoatite contains some relatively large, rounded, colorless inclusions with high relief (white arrows); these were identified as albite by Raman analysis. Several minute, colorless, blocky crystals of xenotime (identified by Raman analysis) were also present in this sample; a few of them are shown here (green arrows). Photomicrograph by John I. Koivula; magnified 15×

Near one of these tourmaline inclusions, a crystal of orangy brown xenotime was identified by Raman analysis (again, see figure 24). In the elbaite portion of another parti-colored sample, xenotime with a quite different appearance was also identified by Raman analysis: minute, colorless, blocky crystals aligned parallel to color zoning (again, see figure 23). Quartz was present in one liddicoatite sample as a relatively large, rounded, colorless inclusion. Black pinpoints (not identifiable) were seen in one parti-colored elbaite sample. Negative crystals and cavities were present in a few samples.

Figure 24. Several prismatic, birefringent inclusions are evident in this parti-colored liddicoatite; the largest one was identified as tourmaline by Raman analysis. The Raman spectrum of the adjacent dark orangy brown inclusion showed that it was xenotime. Photomicrograph by John I. Koivula; partially cross-polarized light, magnified 2.5×.



**TABLE 2.** Chemical composition of liddicoatite from Madagascar.<sup>a</sup>

Chemical composition	Anjanabonoina (probable) <sup>b-1</sup>			Anjanabonoina <sup>b-2</sup>	Anjanabonoina <sup>b-3</sup>	Anjanabonoina <sup>b-4,c,d</sup>		Antsirabe area <sup>b-5,c</sup>
	1.17 ct RSC Dk. bluish green	1.85 ct RSC Colorless	2.84 ct RSC Pale pink	5.47 ct RBC Purplish red	1.05 ct hexagon Purplish red	nr Dk. red	nr Dk. greenish yellow	Holotype specimen Brown
Oxides (wt.%)								
SiO <sub>2</sub>	36.87	37.43	37.12	37.50	37.81	37.58	37.02	37.70
TiO <sub>2</sub>	nd	nd	nd	nd	nd	0.59	0.11	0.38
B <sub>2</sub> O <sub>3</sub>	11.00	11.18	11.03	10.92	11.00	11.36	11.07	10.89
Al <sub>2</sub> O <sub>3</sub>	40.23	41.18	40.06	37.99	38.96	40.22	39.08	37.90
FeO	0.98	0.10	0.12	0.09	nd	0.57	0.74	0.83
MnO	0.34	0.10	0.22	2.84	0.10	0.65	4.86	0.27
MgO	nd	nd	nd	nd	nd	0.07	0.07	0.11
CaO	2.78	3.46	3.84	3.03	4.05	4.00	2.86	4.21
Li <sub>2</sub> O	2.36	2.57	2.63	2.35	2.75	2.85	1.88	2.48
Na <sub>2</sub> O	1.35	0.92	0.79	1.27	0.59	1.72	1.01	0.88
K <sub>2</sub> O	nd	nd	nd	0.04	nd	0.24	0.19	nr
H <sub>2</sub> O	3.16	3.23	3.23	3.77	3.34	3.45	3.44	2.69
F	1.33	1.33	1.22	nr	0.96	0.98	0.81	1.72
Subtotal	100.62	101.54	100.48	99.80	99.72	104.28	103.13	100.06
-O=F	0.56	0.56	0.51	0.00	0.41	0.41	0.34	0.72
Total	100.06	100.98	99.97	99.80	99.32	103.87	102.79	99.34
Ions on the basis of 31 (O,OH,F)								
Si	5.826	5.818	5.846	5.970	5.971	5.750	5.811	6.015
Al	0.174	0.182	0.154	0.030	0.029	0.250	0.189	0.000
Tet. sum	6.000	6.000	6.000	6.000	6.000	6.000	6.000	6.015
B	3.000	3.000	3.000	3.000	3.000	2.999	2.999	2.999
Al (Z)	6.000	6.000	6.000	6.000	6.000	6.000	6.000	6.000
Al	1.318	1.363	1.282	1.099	1.222	1.004	1.042	1.127
Ti	nd	nd	nd	nd	nd	0.068	0.013	0.046
Fe <sup>2+</sup>	0.130	0.013	0.016	0.011	nd	0.073	0.097	0.111
Mn	0.046	0.013	0.029	0.383	0.013	0.084	0.646	0.036
Mg	nd	nd	nd	nd	nd	0.016	0.016	0.026
Li	1.497	1.609	1.663	1.507	1.765	1.755	1.185	1.591
Y sum	3.000	3.000	3.000	3.000	3.000	2.999	3.000	2.937
Ca	0.471	0.576	0.648	0.517	0.685	0.656	0.481	0.720
Na	0.414	0.277	0.241	0.393	0.179	0.510	0.307	0.272
K	nd	nd	nd	0.009	nd	0.047	0.038	nr
Vacancy	0.116	0.146	0.111	0.081	0.136	0.000	0.173	0.008
X sum	1.000	1.000	1.000	1.000	1.000	1.213	1.000	1.000
F	0.665	0.654	0.608	nr	0.481	0.474	0.402	0.868
OH	3.335	3.346	3.392	4.000	3.520	3.526	3.598	2.863
Ca/(Ca+Na)	0.53	0.68	0.73	0.57	0.79	0.56	0.61	0.73

<sup>a</sup>All iron reported as FeO. Except where noted, all analyses were by electron microprobe, with Li<sub>2</sub>O, B<sub>2</sub>O<sub>3</sub>, and H<sub>2</sub>O calculated by stoichiometry: B = 3 apfu (atoms per formula unit), Li = 3-SumY, and OH + F = 4 apfu. Note that some cation sums may not add up exactly as shown, due to rounding of the calculated numbers. Abbreviations: dk. = dark, lt. = light, nd = not detected, nr = not reported, RBC = round brilliant cut, and RSC = rectangular step cut. Nuber and Schmetzer (1981) reported the composition of a green Madagascar liddicoatite as (Ca<sub>0.65</sub>Nb<sub>0.35</sub>)(Li<sub>1.40</sub>Al<sub>1.60</sub>)Al<sub>9</sub>(O,OH,F)<sub>4</sub>(BO<sub>3</sub>)<sub>3</sub>Si<sub>6</sub>O<sub>19</sub>.

<sup>b</sup>Reference/analyst—b-1: F. C. Hawthorne (this study); b-2: Caltech sample 12961; b-3: W. B. Simmons and A. U. Falster; (this study) b-4: Lacroix (1922a); b-5: Dunn et al. (1977); b-6: Duparc et al. (1910); b-7: Akizuki et al. (2001); b-8: Aurisicchio et al. (1999); and b-9: Bloomfield (1997), see also table 5.12, analysis 57 of Shmakin and Makagon (1999). Analyses by F. C. Hawthorne used a Cameca SX 50 instrument, with minerals or synthetic compounds as standards, an accelerating voltage of 15 kV, sample current of 20–30 nA, 10 μm beam diameter, 20–30 second count time, and the data correction procedure of Pouchou and Pichoir (1985); the following elements were analyzed for but not detected: P, Sc, V, Cr, Co, Ni, Cu, Zn, Sb, and Bi. Analyses by W. B. Simmons and A. U. Falster used an ARL SEMQ instrument, with minerals or synthetic compounds as standards, an accelerating voltage of 15 kV, sample current of 15 nA, 2 μm beam diameter, 60 second count time, and the CITZAF φ(ρZ)/PRSUPR data acquisition and data reduction program; the following elements were analyzed for but not detected: V, Cr, Cu, Zn, and Bi, except in the 1.05 ct hexagon which contained up to 0.10 wt.% V<sub>2</sub>O<sub>5</sub>, 0.15 wt.% ZnO, and 0.09 wt.% Bi<sub>2</sub>O<sub>3</sub>.

**Chemical Composition.** Chemical analyses of Madagascar liddicoatite from this study and the literature are presented in table 2. Because of space limitations, only selected analyses are shown; the remainder

of the data (including elbaite analyses) can be viewed on the Internet at the *Gems & Gemology* data depository ([www.gia.edu/gandg/ggDataDepositary.cfm](http://www.gia.edu/gandg/ggDataDepositary.cfm)). As illustrated in figure 25, a considerable portion of

Antaboaka <sup>b-6,c,e</sup>	Maroandro <sup>b-6,c,f</sup>	Jochy <sup>b-7,g</sup>	Lacamisinten <sup>b-8,h</sup>	Malakialina <sup>i</sup>				Sahatany Valley <sup>b-9</sup>
nr Red	nr Pink	Specimen A nr	Crystal section Pink-red	Pink rim	Crystal section Lt. yellow	Lt. green	Darker green	TB01 nr
37.29	37.06	38.31	37.22	37.74	37.96	37.91	37.94	37.47
nr	nr	nd	0.07	0.03	0.36	0.11	0.12	0.08
11.01	11.04	11.10	10.93	10.91	11.04	10.99	11.02	11.19
38.91	40.53	38.57	38.03	37.70	37.92	37.95	38.00	41.08
0.70	0.36	0.02	0.10	0.06	1.14	0.81	1.16	0.29
0.52	1.23	0.05	4.06	0.70	0.22	0.11	0.15	0.20
0.30	0.43	nd	0.18	0.08	0.10	0.10	0.13	nd
4.10	2.58	4.69	2.63	3.95	4.10	4.15	4.16	3.30
2.59	2.10	2.97	1.86	2.80	2.75	2.80	2.75	2.55
0.76	0.80	0.54	1.40	1.00	0.94	0.96	0.95	1.08
0.10	0.13	0.09	0.02	nd	nd	nd	nd	0.02
3.14	3.23	2.78	3.17	2.50	2.67	2.89	2.95	3.46
1.40	1.23	2.21	0.64	2.67	2.40	1.91	1.79	0.84
100.82	100.71	101.33	100.31	100.15	101.60	100.69	101.14	101.57
0.59	0.52	0.93	0.27	1.12	1.01	0.80	0.75	0.35
100.23	100.20	100.40	100.04	99.02	100.59	99.89	100.39	101.22
5.885	5.835	5.999	5.966	6.013	5.976	5.992	5.980	5.817
0.115	0.165	0.001	0.034	0.000	0.024	0.008	0.020	0.183
6.000	6.000	6.000	6.000	6.013	6.000	6.000	6.000	6.000
3.000	3.000	3.000	3.024	3.000	3.000	3.000	3.000	3.000
6.000	6.000	6.000	6.000	6.000	6.000	6.000	6.000	6.000
1.122	1.357	1.118	1.152	1.078	1.013	1.062	1.040	1.333
nr	nr	nd	0.008	0.004	0.042	0.013	0.015	0.009
0.092	0.047	0.003	0.013	0.008	0.150	0.108	0.153	0.038
0.070	0.164	0.007	0.551	0.095	0.029	0.014	0.020	0.026
0.071	0.101	nd	0.043	0.018	0.024	0.025	0.031	nd
1.645	1.331	1.872	1.199	1.797	1.741	1.778	1.741	1.593
3.000	3.000	3.000	2.967	3.000	3.000	3.000	3.000	3.000
0.693	0.435	0.787	0.452	0.674	0.692	0.703	0.702	0.549
0.233	0.244	0.164	0.435	0.310	0.287	0.294	0.289	0.325
0.020	0.026	0.018	0.004	nd	nd	nd	nd	0.004
0.054	0.294	0.031	0.109	0.015	0.020	0.002	0.009	0.122
1.000	1.000	1.000	1.000	1.000	1.000	1.000	1.000	1.000
0.699	0.612	1.095	0.324	1.343	1.194	0.953	0.893	0.412
3.301	3.388	2.905	3.390	2.657	2.806	3.047	3.107	3.588
0.75	0.64	0.83	0.51	0.68	0.71	0.71	0.71	0.63

<sup>c</sup>Determined by wet chemistry.

<sup>d</sup>Spectrographic analysis also revealed traces of Ga and Pb.

<sup>e</sup>This sample had R.I. values of  $n_{\omega} = 1.6411$  and  $n_e = 1.6256$ , birefringence = 0.0155, and S.G. = 3.047.

<sup>f</sup>This sample had R.I. values of  $n_{\omega} = 1.6498$  and  $n_e = 1.6246$ , birefringence = 0.0162, and S.G. = 2.978.

<sup>g</sup>Analysis of the o sector of a sector-zoned crystal.

<sup>h</sup>Average of three analyses; Lacamisinten is the name used by gem dealers, but the actual Malagasy name is Alakamisy Itenina.  $B_2O_3$  was determined by SIMS,  $Li_2O$  by atomic absorption, and  $H_2O$  by GC and TGA.

<sup>i</sup>Unpublished data of W. B. Simmons and A. U. Falster.

<sup>j</sup>Calculation included traces of Pb; this element is not shown above due to possible contamination problems.

the analyses from this study correspond to elbaite compositions. As expected, there was no correlation between color and Ca/Na content.

Among the liddicoatite analyses, Ca contents

ranged from relatively constant to variable (e.g., 2.74–4.56 wt.% CaO in one slice) within single samples. An X-ray map of a small portion of one sample revealed gradational Ca contents that corre-

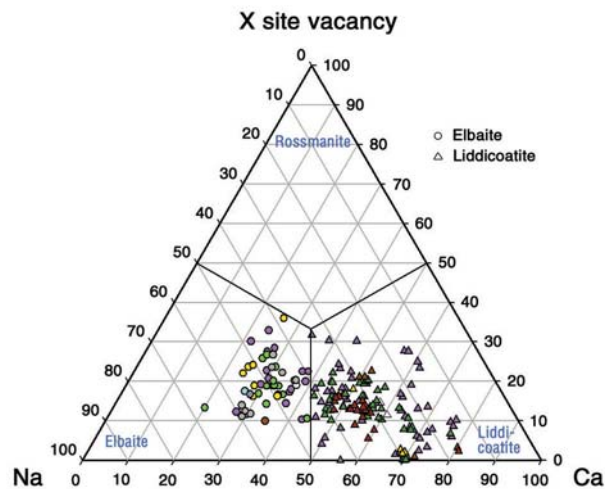


Figure 25. This compositional plot shows the X-site occupancy for the 191 liddicoatite-elbaite analyses from Madagascar obtained for this study and taken from the literature (see table 2 and depository table). The color of each data point is indicative of the color of the tourmaline; points for which no color was reported are shown in dark red. All of the data points fall into the liddicoatite and elbaite fields, and there is no correlation between X-site occupancy and color.

sponded to both liddicoatite and elbaite compositions (figure 26). The most Ca-rich and Na-poor liddicoatite that we know of was published by Akizuki et al. (2001); it contained 4.69 wt.% CaO and 0.54 wt.% Na<sub>2</sub>O (83 mol.% liddicoatite).

The chromophoric elements Fe, Mn, and Ti were typically low in the Madagascar tourmaline. The highest contents of these elements were found in the parti-colored samples; these analyses can be viewed in the data depository. Up to 2.66 wt.% FeO was measured (in a pale gray zone), and the green and blue zones had significantly more iron than the colorless or pink bands (again, see figure 26). High Mn contents were reported for a dark greenish yellow sample analyzed by Lacroix (1922a) that contained 4.86 wt.% MnO, and for some of the purplish red stones analyzed for this study (up to 3.22 wt.% MnO). The greatest Ti content was measured in a yellow color zone: 0.82 wt.% TiO<sub>2</sub>. Fluorine contents were typically above 1 wt.%. Traces of Mg, K, and Pb also were present, although backscatter electron imaging of some samples revealed surface contamination of pores and fractures with lead (Pb). Therefore all of the Pb analyses of our samples are considered unreliable and are not reported in the data. The Pb residue probably resulted from the polishing process used by the lapidary (J. Zang, pers. comm., 2002). This element

has not been included in analyses of liddicoatite published in the literature.

For chemical data on liddicoatite from other world localities, see Appendix A.

## DISCUSSION

**Color Zoning.** Benesch (1990) provided a detailed description of color zoning in Madagascar tourmaline, with excellent illustrations of cross-sections cut in orientations perpendicular and parallel to the c-axis (see, e.g., figure 27). A visual journey through a succession of liddicoatite slices cut perpendicular to the c-axis is accessible on the Internet at [minerals.gps.caltech.edu/mineralogy/animation.htm](http://minerals.gps.caltech.edu/mineralogy/animation.htm).

The slices we studied displayed color zoning that is consistent with the features described for liddicoatite by Dunn et al. (1977, 1978). These authors (as well as earlier researchers) indicated that, while the color zoning in elbaite is parallel to the basal pinacoid and/or prism faces, the predominant triangular color boundaries in liddicoatite are "parallel to

Figure 26. This X-ray map, generated with an electron microprobe by one of the authors (WS), shows the distribution of Ca and Fe in a portion of the 1.29 ct freeform sample. Point analyses by the microprobe showed that the darker green (i.e., Ca-rich) area on the lower right of the X-ray map is liddicoatite, and the lighter green area on the upper left is elbaite. The red bands in the X-ray map show enrichment in Fe, and correspond to the dark bluish green layers in the sample.



a pyramid." Therefore, in slices cut perpendicular to the c-axis, these boundaries will not appear sharp. In contrast, the outer concentric color zones are parallel to prism faces (and thus the c-axis), so they do appear sharp in the slices (see, e.g., figure 1). Regardless of which color zones are observed, both abrupt and gradual transitions from one color to another are seen; these reflect dynamic geochemical changes in the crystallization environment (Lacroix, 1922a; Benesch, 1990; Zang, 2000).

Although not seen in our study samples, a trigonal star pattern is a notable feature of many Madagascar tourmaline slices cut perpendicular to the c-axis (e.g., Lacroix, 1922a; Wentling, 1980; Zang, 1994c). This star is typically pink or red, and crosscuts the adjacent triangular zones before being truncated against the outer concentric color layers (see figure 3). In slices cut *parallel* to the c-axis (figure 27), this same feature may be visible as a spike-shaped color zone of variable width that follows the apex of the pyramidal faces. Trigonal stars of various colors have been seen in tourmaline from Brazil, Mozambique, and elsewhere, although these crystals are typically smaller (less than 4 cm in diameter) than those from Madagascar (Benesch, 1990); we did not chemically analyze any such samples for this study. The origin of these stars has been debated for years (Benesch, 1990). From his observations of Madagascar tourmaline, Zang (1994c) suggested that during crystallization under decreasing temperature, the red stars form as a result of the preferential incorporation of the large  $Mn^{2+}$  ion into the fast-growing pyramid {1011} faces.

Another color-zoning phenomenon (not seen in our study samples but found in some tourmalines from Madagascar, Brazil, and Namibia) is the "aggregate type" zoning described by Benesch (1990). This is present in crystal portions (generally near the termination) that consist of an accumulation of tourmaline subcrystals in parallel orientation. Slices cut from such crystals often display spectacular mottled patterns (see, e.g., figure 14).

**Gemological Properties.** As in elbaite, the R.I. values of liddicoatite should vary with transition metal contents (e.g., Fe, Mn, and Ti): Higher contents of these elements lead to greater R.I. and birefringence values (Deer et al., 1997). Although in most cases we could not obtain R.I. measurements on the narrow individual color zones, for those few samples with wide enough color zones, the lack of systematic R.I. trends was probably due to the relatively



Figure 27. This watercolor painting of an Anjanabonoina tourmaline sliced parallel to the c-axis shows how the color zoning is oriented parallel to the prism and pyramid faces. Note also the central spike-shaped pink area that follows the apex of the pyramidal faces. Looking perpendicular to the c-axis, this pink zone would form the central part of a trigonal star. This cross-section was reconstructed from a series of slices from the same crystal oriented perpendicular to the c-axis. Reprinted with permission from Benesch (1990, p. 298), © Verlag Freies Geistesleben & Urachhaus GmbH, Stuttgart, Germany.

small variations in overall transition metal contents. From a study of several tourmalines of different colors and from different deposits in Madagascar, Lacroix (1922a) noted a general correlation between increasing R.I. and S.G. values, but no systematic relationship of either measurement to color. The R.I. values we measured (1.619–1.651) were similar to the range Lacroix reported (1.6200–1.6480) but somewhat higher than those reported by Dunn et al. (1978) for liddicoatite (1.621 and 1.637,  $\pm 0.003$ ). The birefringence values we obtained (0.014–0.027) are fairly similar to those of Lacroix (0.0162–0.0236).

The slabs (cut perpendicular to the c-axis) apparently contained biaxial domains, as they yielded two R.I. values with significant birefringence (i.e., up to 0.027). Lacroix (1922a) noted that Madagascar tourmaline crystals are locally biaxial; however, he observed no correlation between biaxial character and color zoning. In liddicoatite from Jochy, Madagascar, Akizuki et al. (2001) determined that biaxial domains—which have triclinic and orthorhombic symmetry—correspond to certain crystallographic sectors (and compositional zoning) that formed during crystal growth. Biaxial domains also have been found in elbaite (see Foord and Mills, 1978). The common occurrence of strain patterns in elbaite and liddicoatite may therefore be related to biaxial domains that formed during growth.

Notwithstanding the effects of inclusions, the specific gravity of tourmaline increases with greater contents of transition metals (Deer et al., 1997). Our multicolored samples showed rather small variations in specific gravity (3.05–3.07). The higher S.G. values (3.06–3.11) obtained for the eight purplish red liddicoatites may be due to the fact that they contained fewer fluid inclusions than the multicolored samples. There was no systematic relationship between transition-metal content and S.G. in our samples. The S.G. values of the multicolored samples fell within the ranges reported for tourmaline of liddicoatite composition: 3.052–3.092 (Lacroix, 1922a) and 3.00–3.07 (Dunn et al., 1978). The higher S.G. values measured for the purplish red samples are consistent with the 3.107 value reported by Lacroix (1922a) for “amethyst”-violet tourmaline from Anjanabonoina.

The partially healed fractures, feathers, tubes, and pinpoints seen in our study samples are typical of inclusions in tourmaline (see, e.g., Webster, 1994). Among the mineral inclusions, albite and tourmaline are commonly found in elbaite (see

Koivula, 1994; Webster, 1994). To our knowledge, however, xenotime and quartz had not been documented previously in elbaite or liddicoatite.

**Chemical Properties.** To distinguish liddicoatite from elbaite, cations in the formula are calculated from the weight-percent oxides obtained from the quantitative chemical analyses so that the X-site constituents can be compared on an “atoms per formula unit” basis. In an analysis of lithium tourmaline, if Ca is the dominant element in the X site, it is liddicoatite. Conversely, elbaite is the Na-dominant species. Besides Ca and Na, this site may contain potassium and/or vacancies. Although potassium is not important in tourmaline, vacancies may constitute a significant proportion of the X site; if they are dominant, then the lithium tourmaline species is rossmanite. (For more on distinguishing among lithium-aluminum tourmalines, see Hawthorne and Henry [1999] and Zolotarev and Bulakh [1999].)

Dunn et al. (1978) indicated that Madagascar tourmaline crystals usually are composed entirely of one species. This was not the case for several of the samples we analyzed from Madagascar and elsewhere (see depository data). Akizuki et al. (2001) studied two sector-zoned liddicoatite crystals from Jochy, Madagascar, one of which contained elbaite in the  $a\{11\bar{2}0\}$  sector. Nevertheless, some liddicoatite from Madagascar is chemically homogeneous enough to be used as a reliable reference material for elemental and isotopic work (Aurischio et al., 1999). The experience of one of the authors (FP) has shown that the polychrome crystals from Anjanabonoina usually are derived from large cavities, and these tourmalines are typically liddicoatite throughout. By contrast, crystals showing simpler zonation from small cavities at this mine are predominantly elbaite or dravite, with liddicoatite being scarce or absent.

The Ca and Na contents of liddicoatite show no systematic relationship to color (Dunn et al., 1978; see also figure 25). Conversely, Fe, Mn, and Ti affect the coloration of liddicoatite in the same way that they affect elbaite (Dietrich, 1985). Analyses of colorless samples revealed very small amounts of these elements. Pink samples contained small but significant amounts of Mn and very low amounts of Fe, whereas green portions contained higher Fe; analogous trends were reported by Webber et al. (2002) in liddicoatite from Anjanabonoina and Fianarantsoa. Yellow bands generally have moderately low to low

---

Fe with higher Mn and Ti. The blue, greenish blue, and gray portions contained the highest Fe. The coloration of elbaite (and liddicoatite, by inference) is well documented in the literature; for useful reviews, see Althaus (1979), Dietrich (1985), Zang (1994a), Deer et al. (1997), and the Web site [minerals.caltech.edu/files/visible/tourmaline/index.htm](http://minerals.caltech.edu/files/visible/tourmaline/index.htm).

**Geologic Origin.** Selway et al. (1999) noted that liddicoatite may be found in elbaite-subtype pegmatites, but not in those of the lepidolite subtype. Selway (1999) indicated that within elbaite-subtype pegmatites, liddicoatite-elbaite is the last tourmaline to form (i.e., after the crystallization of Ca-bearing schorl and Mn-rich elbaite). Therefore, geochemically it is the most “evolved” tourmaline in these pegmatites.

Granitic pegmatites typically are not rich in Ca, and any amounts present may be consumed by the early crystallization of plagioclase and Ca-bearing tourmaline. The presence of liddicoatite in gem-bearing cavities indicates that Ca was abundant during late-stage pegmatite crystallization. Teertstra et al. (1999) postulated that the Ca needed to form liddicoatite could be mobilized from the pegmatite host rocks or the alteration of previously crystallized Ca-bearing minerals (e.g., plagioclase), or the Ca could be geochemically conserved (e.g., as fluoride complexes) during pegmatite crystallization until late stages. While all three of these mechanisms may play a role, it is important to note that in elbaite-subtype pegmatites, liddicoatite is typically found in deposits that are located in or near Ca-rich host rocks (Selway, 1999). (One exception is liddicoatite from the Malkhan district in Russian, which is not associated with Ca-rich host rocks.) Although Ca-rich minerals are common in many Madagascar pegmatites, liddicoatite is not always present and therefore its formation may be related more to paragenetic effects (i.e., pertaining to the order of mineral crystallization) than to the total amount of Ca available in the pegmatite system.

A petrogenetic model for the formation of the Anjanabonoina pegmatites is currently being developed (Dini et al., 2002; De Vito, 2002; and unpublished work of one of the authors [FP]). This model invokes significant contamination of the pegmatitic melts with components derived from the metasedimentary (including dolomitic carbonate) host rocks. Isotopic data suggest that the boron in the pegmatites is derived from metasedimentary evaporitic rocks. In this model, the pegmatitic magmas formed

by the fractional crystallization of late to post-tectonic granites—and were contaminated by fluids derived from the metasediments of the Itremo Group—during pegmatite emplacement in extensional faults. The complex color zoning of the polychrome tourmaline reflects a dynamic multistage crystallization process.

## IDENTIFICATION

Dunn et al. (1977) reported that liddicoatite cannot be differentiated from elbaite by its optical and physical characteristics, or even with X-ray diffraction techniques and unit cell dimension data. In the gem trade, liddicoatite traditionally has been informally separated from elbaite by the presence of features such as triangular color zoning, a trigonal star, or parti-colored zonation. However, quantitative chemical analyses are required to confirm the tourmaline species. Since they cannot be separated by practical gemological methods, gemologists typically do not distinguish between liddicoatite and elbaite. Therefore, some tourmalines sold as elbaite may actually be liddicoatite, and more localities for this species are being recognized as chemical analyses are obtained (see, e.g., Hlava, 2001; Laurs, 2001; Appendix A).

Little is known about the treatments done to liddicoatite. We could not find any reference to the heating or irradiation of this tourmaline, although some “elbaite” treated by these methods may actually be liddicoatite, as discussed above. Reddish violet tourmaline (probably liddicoatite) from the Coronel Murta area in Minas Gerais, Brazil, has been heat-treated to a green color (H. Elawar, pers. comm., 2002). A polychrome tourmaline slice (locality not specified) was recently reported to be fracture-filled with resin (Bank et al., 1999b). Madagascar tourmaline slices containing natural fractures are commonly stabilized with resin (W. Larson, pers. comm., 2002). Fractured slices also have been stabilized by constructing doublets with glass or plastic (Koivula et al., 1992; Henn and Bank, 1993; Bank et al., 1999a).

Wax or oil was tentatively identified in some slices obtained for this study. According to W. Larson (pers. comm., 2002), prior to polishing the slices, surface irregularities are filled with paraffin wax to prevent the unsightly concentration of polishing residues in those areas. The wax is then melted away by boiling the slices in water, although it is not always completely removed from the fractures.



Figure 28. Designers enjoy incorporating the beautiful banding of liddicoatite into creative carvings. The butterfly brooch shown here is made of 18K yellow and white gold with two carved Madagascar tourmalines (84.47 ct total weight), yellow and colorless diamonds, and pearls. Courtesy of Buccellati.

## CONCLUSION

Most of the liddicoatite in the gem trade has come from the Anjanabonoina pegmatites in central Madagascar. Although fine color-zoned tourmalines have been recovered elsewhere in the world, and some of these have been identified as liddicoatite by quantitative chemical analysis, the complex color zones and patterns seen in Madagascar tourmaline

are unrivaled by tourmaline from other localities (Benesch, 1990). The difficult access, mining conditions, and security problems continue to limit further production at Anjanabonoina, although previously mined material does enter the market occasionally. Dramatic and unusual, liddicoatite is revered by gem collectors and researchers, and is well-suited for one-of-a-kind jewelry designs (figure 28).

### ABOUT THE AUTHORS

Ms. Dirlam (ddirlam@gia.edu) is director of the Richard T. Liddicoat Library and Information Center, and Mr. Laurs is senior editor of *Gems & Gemology* at GIA in Carlsbad. Dr. Pezzotta is curator of mineralogy at the Museo Civico di Storia Naturale, Milan, Italy. Dr. Simmons is professor of mineralogy in the Department of Geology and Geophysics at the University of New Orleans, Louisiana.

**ACKNOWLEDGMENTS:** The authors thank Eckehard Julius Petsch of Julius Petsch Jr., Idar-Oberstein, Germany, for providing information on the history and mining of the Anjanabonoina pegmatite. Electron microprobe analyses were performed by Dr. Frank Hawthorne and Ron Chapman at the University of Manitoba, Winnipeg, Canada, and by one of the authors (WS) and Alexander U. Falster at the University of New Orleans, Louisiana. John I. Koivula of the GIA Gem Trade Laboratory in Carlsbad performed photomicrography, and Shane Elen and Sam Muhlmeister of GIA provided helpful assistance with Raman analyses. Samples of tourmaline were provided for this study by William Larson (Pala International, Fallbrook, California), Tom Cushman (Allerton Cushman & Co., Sun Valley, Idaho), Benjamin Rondeau (National Museum of Natural History, Paris),

Richard T. Liddicoat (GIA, Carlsbad), John Patrick (El Sobrante, California), and the GIA collection. We thank the following for assistance with translating selected publications: Inna Saphonova (Novosibirsk, Russia), Valerie Chabert (formerly of the GIA Gem Trade Laboratory in New York), Sheryl Elen (GIA Library, Carlsbad), and Claus Hedegaard (Roende, Denmark). Neil Barron (GIA Library, Carlsbad) is thanked for obtaining numerous publications via interlibrary loan. Dr. Julie Selway (Ontario Geological Survey, Sudbury, Ontario, Canada) provided helpful discussions on tourmaline composition. Hassaim Elawar (K. Elawar Ltda., Teófilo Otoni, Brazil) and Dr. Anthony Kampf (Natural History Museum of Los Angeles County, Los Angeles, California) provided information on liddicoatite from Brazil. Dr. Milan Novák (Moravske Zemske Muzeum, Brno, Czech Republic) supplied information on liddicoatite from this country. Dr. Kampf, Dr. Joachim Zang (Gustav Zang, Idar-Oberstein, Germany), Dr. Emmanuel Fritsch (Institut des Matériaux de France in Nantes), and Dr. Alfred Levinson (University of Calgary, Alberta, Canada) are thanked for their constructive reviews of this manuscript.

Special thanks to Richard Liddicoat for his encouragement and advice on this article, and for his lifelong contributions to colored stone research.

## APPENDIX A: WORLD SOURCES OF LIDDICOATITE

In addition to Anjanabonoina, liddicoatite has been identified from several locations in central and south-central Madagascar, including Antaboaka, Jochy, Lacamisinten (also called Alakamisy Itenina), Malakialina, Maroandro, and the Sahatany Valley (see table 2), as well as Vohitrakanga (preliminary data of FP). Table A-1 contains chemical analyses of liddicoatite from elsewhere in the world. All of these localities have produced gem-quality tourmaline except for those in Canada and the Czech Republic, which are included for completeness. In Canada, liddicoatite was found in the High Grade Dike of the Cat Lake–Winnipeg River pegmatite field (Teertstra et al., 1999). The tourmaline occurs at two localities in the Czech Republic. Liddicoatite-elbaite from Bližná in southern Bohemia was documented by Novák et al. (1999). At Recice, liddicoatite is very rare, forming narrow zones in crystals of Ca,Mn-rich elbaite (M. Novák, pers. comm., 1999).

Brazil has been rumored as a possible source of liddicoatite for years (see, e.g., Koivula and Kammerling, 1990; figure A-1). The large faceted stone described in that Gem News item, as well as a 3.95 ct sample from the same source, were confirmed as liddicoatite for this study. Several additional brownish purple Brazilian samples, from the same source (Mauro de Souza, Marcelo Gemas Inc., Los Angeles) were qualitatively analyzed by GIA Research in 1990, and indicated as liddicoatite and elbaite. These samples probably came from the Coronel Murta area, where significant amounts of similar-colored tourmaline have been mined and sold as liddicoatite (H. Elawar, pers. comm., 2002).

Multicolored slices of tourmaline that are reportedly from the “Congo” were analyzed for this study and found to contain liddicoatite in certain zones (without any particular trend in color or position). To our knowledge, this is the first time liddicoatite has been identified there.

An analysis of liddicoatite from Mozambique was presented by Sahama et al. (1979). Chemical data on tourmaline from this country are uncommon in the literature, and more analyses will probably reveal additional liddicoatite from the extensive pegmatite fields there.

Recently, Nigeria has emerged as a source of liddicoatite. Electron microprobe analyses of an orangy pink liddicoatite from the Ogbomosho area revealed relatively high bismuth contents (Hlava, 2001), and a purplish red crystal from the Abuja area was also confirmed as liddicoatite (Laurs, 2001, and this study). Further analyses of multicolored slices from Nigeria done for this study revealed liddicoatite in

several samples and representing many colors (see depository data).

Liddicoatite has been documented from the Malkan district in Russia (see Zagorsky et al., 1989; Zagorsky and Peretyazhko, 1992). A sample analyzed from the Transbaikalia area for this study contained zones of liddicoatite, elbaite, and schorl-elbaite.

Zang (1994b) analyzed a tourmaline from Sanga-Sanga, Tanzania, that contained attractive triangular color zones; both liddicoatite and elbaite (as well as schorl) were present in the sample.

Ngu (2001) presented an X-ray diffraction pattern and Raman spectrum for what was reportedly black liddicoatite from Luc Yen, Vietnam, but did not provide a chemical analysis of the material to confirm the identification. A multicolored slice from Vietnam analyzed for this study contained liddicoatite in a red zone. This slab displayed the trigonal star that is so commonly seen in Madagascar liddicoatite, yet it was dominantly elbaite.



Figure A-1. The purplish red color of this rough and cut tourmaline is similar, yet the crystal (elbaite-liddicoatite) is from Anjanabonoina and the oval brilliant (liddicoatite) was reportedly mined in Minas Gerais, Brazil. The crystal (6.4 × 3.7 cm) is courtesy of William Larson, and the faceted stone (20.47 ct) is from the GIA collection. Photo © Harold & Erica Van Pelt.

**TABLE A-1.** Chemical composition of liddicoatite from localities other than Madagascar.<sup>a</sup>

Chemical Composition	Minas Gerais, Brazil <sup>b-1</sup>		Manitoba, Canada <sup>b-2,c</sup>	"Congo" <sup>b-3,d</sup>		Bližná, Czech Republic (Unit A) <sup>b-4,c</sup>	Muiiane, Mozambique <sup>b-5</sup>	Abuja, Nigeria <sup>b-3,e</sup>
	20.37 ct cushion Purplish red	3.95 ct cushion Purplish red	nr	Slice	Slice	nr	nr	1.39 ct crystal
			nr	Grayish pink	Yellowish green	Pink	Brown	Purplish red
Oxides (wt.%)								
SiO <sub>2</sub>	38.08	37.27	37.20	37.68	38.53	35.50	36.55	38.45
TiO <sub>2</sub>	nr	nr	nr	0.03	0.05	0.34	0.07	nd
B <sub>2</sub> O <sub>3</sub>	11.10	10.93	10.84	11.00	11.02	10.84	10.87	11.23
Al <sub>2</sub> O <sub>3</sub>	39.81	38.71	40.70	39.26	37.94	38.30	38.45	40.15
FeO	0.00	0.11	0.30	0.46	0.68	0.14	2.94	0.09
MnO	0.29	2.39	1.50	0.60	0.57	4.62	0.77	0.22
MgO	nr	nr	nr	nd	nd	0.05	0.16	0.05
CaO	3.25	2.79	2.50	3.53	3.13	2.58	2.88	3.02
Li <sub>2</sub> O	2.62	2.28	2.03	2.51	2.79	1.66	2.13	2.69
Na <sub>2</sub> O	0.97	1.30	1.20	0.57	1.09	1.39	1.42	1.48
K <sub>2</sub> O	nr	nr	nr	nd	nd	nr	nd	0.02
H <sub>2</sub> O	3.13	3.08	3.37	3.54	3.59	3.07	3.07	3.29
F	1.48	1.45	0.90	0.54	0.45	1.13	1.44	1.23
Subtotal	100.88	100.92	100.54	99.75	99.86	99.62	100.76	101.94
-O=F	0.62	0.61	0.38	0.23	0.19	0.48	0.61	0.52
Total	100.25	100.31	100.16	99.52	99.68	99.14	100.16	101.42
Ions on the basis of 31 (O,OH,F)								
Si	5.961	5.926	5.868	5.951	6.078	5.765	5.842	5.951
Al	0.039	0.074	0.132	0.049	0.000	0.235	0.158	0.049
Tet. sum	6.000	6.000	6.000	6.000	6.078	6.000	6.000	6.000
B	3.000	3.000	2.952	3.000	3.000	3.039	3.000	3.000
Al (Z)	6.000	6.000	6.000	6.000	6.000	6.000	6.000	6.000
Al	1.306	1.181	1.434	1.260	1.054	1.097	1.085	1.275
Ti	nr	nr	nr	0.004	0.005	0.042	0.008	0.000
Fe <sup>2+</sup>	0.000	0.015	0.040	0.061	0.089	0.019	0.393	0.011
Mn	0.038	0.322	0.200	0.080	0.076	0.636	0.104	0.029
Mg	nr	nr	nr	nd	nd	0.012	0.038	0.011
Li	1.649	1.457	1.288	1.592	1.771	1.084	1.371	1.674
Y sum	3.000	3.000	2.962	3.000	3.000	2.890	3.000	3.000
Ca	0.545	0.475	0.423	0.597	0.529	0.449	0.493	0.500
Na	0.294	0.401	0.367	0.174	0.333	0.438	0.440	0.445
K	nr	nr	nr	nd	nd	nr	nd	0.004
Vacancy	0.160	0.124	0.210	0.229	0.138	0.113	0.065	0.051
X sum	1.000	1.000	1.000	1.000	1.000	1.000	1.000	1.000
F	0.733	0.729	0.449	0.270	0.222	0.580	0.728	0.603
OH	3.267	3.270	3.546	3.730	3.778	3.326	3.272	3.397
Ca/(Ca+Na)	0.65	0.54	0.54	0.77	0.61	0.51	0.53	0.53

<sup>a</sup>All iron reported as FeO. Except where noted, all analyses by electron microprobe, and Li<sub>2</sub>O, B<sub>2</sub>O<sub>3</sub>, and H<sub>2</sub>O calculated by stoichiometry: B = 3 apfu (atoms per formula unit), Li = 3-SumY, and OH + F = 4 apfu. Note that some cation sums may not add up exactly as shown, due to rounding of the calculated numbers. Abbreviations: lt. = light, nd = not detected, nr = not reported, xl = crystal.

<sup>b</sup>Reference/analyst—b-1: F. C. Hawthorne (this study); b-2: Teertstra et al. (1998); b-3: W. B. Simmons and A. U. Falster (this study); b-4: Novak et al. (1999); b-5: Sahama et al. (1979); b-6: Zagorsky et al. (1989); and b-7: Zang (1994b). For instrumental operating conditions used by F. C. Hawthorne, as well as by W. B. Simmons and A. U. Falster, see table 2, footnote b.

<sup>c</sup>Average of an unspecified number of analyses; boron, lithium, and hydrogen were determined by ion microprobe (SIMS).

## REFERENCES

Akizuki M., Kuribayashi T., Nagase T., Kitakaze A. (2001) Triclinic liddicoatite and elbaite in growth sectors of tourmaline from Madagascar. *American Mineralogist*, Vol. 86, pp. 364–369.

Althaus K.E. (1979) Wassermelonen und Mohrenköpfe. *Lapis*, Vol. 4, No. 1, pp. 8–11.

Althaus U., Glas M. (1994) Hätte Ikaros einen Turmalin gehabt... *extraLapis* No. 6, Turmalin, pp. 70–71.

Ashwal L.D., Tucker R.D. (1999) Geology of Madagascar: A brief

Nigeria <sup>b-3,f</sup>			Malkhan, Russia <sup>b-6,g</sup>	Transbaikalia, Russia <sup>b-1</sup>	Sanga Sanga, Tanzania <sup>b-7,h</sup>			Vietnam <sup>b-3,i</sup>
Slice			nr	Crystal fragment	Crystal section			Slice
Pinkish orange	Colorless	Lt. pink	Lt. green	Lt. pink	Blue	"Rose"	Yellow-brown	Red
37.90	38.90	38.76	37.85	37.96	37.41	37.12	38.37	36.54
nd	nd	nd	0.09	nr	0.08	0.02	0.02	0.02
10.98	10.98	10.93	11.70	11.12	10.78	10.89	11.05	10.95
39.06	37.47	37.18	38.10	40.23	37.37	39.14	38.76	41.02
0.22	0.05	0.02	0.92	0.17	0.24	0.09	0.11	0.11
0.66	0.36	0.27	1.00	0.58	2.20	1.25	1.01	1.46
nd	nd	nd	0.03	nr	nd	nd	nd	0.04
3.09	3.08	3.20	3.20	2.58	2.58	2.66	2.73	2.04
1.67	3.06	3.10	2.13	2.48	2.40	2.39	2.62	2.04
1.03	0.89	0.83	1.28	1.40	1.31	1.32	1.30	1.08
nd	nd	nd	0.09	nr	nd	0.02	nd	0.02
3.46	3.46	3.47	2.80	3.18	3.65	3.38	3.81	3.32
0.69	0.69	0.63	1.00	1.39	0.15	0.79	0.00	0.98
<u>98.78</u>	<u>98.94</u>	<u>98.43</u>	<u>100.19</u>	<u>101.16</u>	<u>98.17</u>	<u>99.07</u>	<u>99.79</u>	<u>99.61</u>
<u>0.29</u>	<u>0.29</u>	<u>0.27</u>	<u>0.42</u>	<u>0.59</u>	<u>0.06</u>	<u>0.33</u>	<u>0.00</u>	<u>0.41</u>
98.49	98.65	98.16	99.77	100.57	98.11	98.74	99.79	99.20
5.988	6.160	6.165	6.015	5.931	6.032	5.923	6.037	5.799
<u>0.012</u>	<u>0.000</u>	<u>0.000</u>	<u>0.000</u>	<u>0.069</u>	<u>0.000</u>	<u>0.077</u>	<u>0.000</u>	<u>0.201</u>
6.000	6.160	6.165	6.015	6.000	6.032	6.000	6.037	6.000
3.000	3.000	3.000	3.209	3.000	3.000	3.000	3.000	3.000
6.000	6.000	6.000	6.000	6.000	6.000	6.000	6.000	6.000
1.263	0.994	0.971	1.136	1.340	1.103	1.284	1.188	1.472
nd	nd	nd	0.011	nr	0.010	0.002	0.002	0.002
0.029	0.007	0.003	0.122	0.022	0.032	0.012	0.014	0.015
0.089	0.048	0.037	0.135	0.077	0.300	0.169	0.135	0.196
nd	nd	nd	0.007	nr	nd	nd	nd	0.009
<u>1.619</u>	<u>1.951</u>	<u>1.986</u>	<u>1.361</u>	<u>1.558</u>	<u>1.555</u>	<u>1.533</u>	<u>1.660</u>	<u>1.305</u>
3.000	3.000	3.000	2.772	3.000	3.000	3.000	3.000	3.000
0.524	0.522	0.546	0.545	0.432	0.446	0.455	0.460	0.347
0.317	0.274	0.257	0.394	0.424	0.410	0.408	0.397	0.333
nd	nd	nd	0.018	nr	nd	0.004	nd	0.003
<u>0.159</u>	<u>0.205</u>	<u>0.197</u>	<u>0.043</u>	<u>0.144</u>	<u>0.143</u>	<u>0.133</u>	<u>0.141</u>	<u>0.316</u>
1.000	1.000	1.000	1.000	1.000	1.000	1.000	1.000	1.000
0.346	0.346	0.317	0.503	0.687	0.076	0.399	0.000	0.489
3.654	3.654	3.683	2.968	3.313	3.924	3.601	4.000	3.511
0.62	0.66	0.68	0.58	0.50	0.52	0.53	0.54	0.51

<sup>a</sup>Also contained up to 0.10 V<sub>2</sub>O<sub>5</sub>.

<sup>e</sup>Also contained up to 0.09 wt.% ZnO and 0.04 wt.% Bi<sub>2</sub>O<sub>3</sub>; Cl, Cr, V, and Ba were not detected.

<sup>f</sup>Also contained up to 0.04 V<sub>2</sub>O<sub>5</sub>.

<sup>g</sup>Boron and lithium were determined by wet chemistry.

<sup>h</sup>Analyzed by SEM-EDS.

<sup>i</sup>Also contained up to 0.19 wt.% ZnO.

<sup>j</sup>Calculation included traces of Pb; this element is not shown above due to possible contamination problems.

outline. *Gondwana Research*, Vol. 2, No. 3, pp. 335–339.  
 Aurisicchio C., Demartin F., Ottolini L., Pezzotta F. (1999) Homogeneous liddicoatite from Madagascar: A possible reference material? First EMPA, SIMS and SREF data. *European Journal of Mineralogy*, Vol. 11, pp. 237–242.

Bancroft P. (1984) *Gem & Crystal Treasures*. Western Enterprises/Mineralogical Record, Fallbrook, CA.  
 Bank H., Henn U., Milisenda C.C. (1999a) Gemmological News: Tourmaline-plastic-doublet. *Gemmologie: Zeitschrift der Deutschen Gemmologischen Gesellschaft*, Vol. 48, No.

- 1, pp. 6–7.
- Bank H., Henn U., Milisenda C.C. (1999b) Gemmological News: Tourmalines with artificial fracture fillings. *Gemmologie: Zeitschrift der Deutschen Gemmologischen Gesellschaft*, Vol. 48, No. 1, pp. 5–7.
- Bariand P., Poirot J.-P. (1992) *The Larousse Encyclopedia of Precious Gems*. Van Nostrand Reinhold, New York.
- Becker G. (1971) 70 pound tourmaline crystal produces multicolored slabs. *Lapidary Journal*, Vol. 25, No. 1, pp. 72–73.
- Benesch F. (1990) *Der Turmalin*. Verlag Urachhaus, Stuttgart, Germany, 380 pp.
- Besairie H. (1966) Gîtes minéraux de Madagascar. *Annales Géologiques de Madagascar*, No. 34, Tananarive.
- Bloomfield M.J. (1997) Gem Tourmaline Pegmatite Deposits. M.Sc. thesis, Department of Geology, University of Leicester, England.
- Černý P. (1991) Rare-element granitic pegmatites. Part 1: Anatomy and internal evolution of pegmatite deposits. *Geoscience Canada*, Vol. 18, No. 2, pp. 49–67.
- Collins A.S. (2000) The tectonic evolution of Madagascar: Its place in the East African Orogen. *Gondwana Research*, Gondwana Newsletter section, Vol. 3, No. 4, pp. 549–552.
- Dabren A. (1906) Les pierres précieuses a Madagascar. *Bulletin Économique de Madagascar*, Tananarive, Sixth year, No. 4, pp. 327–339.
- De Vito C. (2002) Il Giacimento Gemmifero e ad Elementi Rari dell'Anjanabonoina, Betafo, Madagascar Centrale. Ph.D. dissertation, University "La Sapienza," Rome, Italy.
- Deer W.A., Howie R.A., Zussman J. (1992) *An Introduction to the Rock-Forming Minerals*. Longman Scientific & Technical, Essex, England.
- Deer W.A., Howie R.A., Zussman J. (1997) *Rock-forming Minerals—Disilicates and Ring Silicates*, Vol. 1B, 2nd ed. The Geological Society, London, pp. 559–602.
- Dietrich R.V. (1985) *The Tourmaline Group*. Van Nostrand Reinhold, New York, 300 pp.
- Dini A., Tonarini S., Pezzotta F., De Vito C. (2002) Boron isotope systematics in some pegmatites of the Itremo Group, central Madagascar. Submitted to *Chemical Geology*.
- Dissanayake C.B., Chandrajith R. (1999) Sri Lanka–Madagascar Gondwana linkage; Evidence for a Pan-African mineral belt. *Journal of Geology*, Vol. 107, pp. 223–235.
- Dunn P.J., Appleman D.E., Nelen J.E. (1977) Liddicoatite, a new calcium end-member of the tourmaline group. *American Mineralogist*, Vol. 62, pp. 1121–1124.
- Dunn P.J., Nelen, J.E., Appleman, D.E. (1978) Liddicoatite, a new gem tourmaline species from Madagascar, *Journal of Gemmology*, Vol. 16, No. 3, pp. 172–176.
- Duparc L., Wunder M., Sabot R. (1910) Les minéraux des pegmatites.—Les tourmalines. Chapter 11 in *Les Minéraux des Pegmatites des Environs d'Antsirabé a Madagascar*, *Mémoires de la Société de Physique et d'Histoire Naturelle de Genève*, Vol. 36, No. 3, pp. 381–401.
- Fernandez A., Huber S., Schreurs G. (2000) Evidence for Late Cambrian–Ordovician final assembly of Gondwana in central-Madagascar. *Summit 2000*, Geological Society of America Annual Meeting, Reno, NV, November 13–16, p. A-175.
- Fernandez A., Huber S., Schreurs G., Villa I., Rakotondrzafy M. (2001) Tectonic evolution of the Itremo region (central Madagascar) and implications for Gondwana assembly. *Gondwana Research*, Vol. 4, No. 2, pp. 165–168.
- Foord E.E., Mills B.A. (1978) Biaxiality in 'isometric' and 'dimetric' crystals. *American Mineralogist*, Vol. 63, pp. 316–325.
- Frondel C. (1946) Tourmaline pressure gauges. *Geological Society of America Bulletin*, Vol. 57, Pt. 2, pp. 1194–1195.
- Giraud P. (1957) Les principaux champs pegmatitiques de Madagascar. *Comptes Rendus—Géologie Conférence de Tananarive*, Commission de Coopération Technique en Afrique au Sud du Sahara, Service Géologique de Madagascar, pp. 139–150.
- Goldschmidt V. (1923) *Atlas der Krystallformen*. Carl Winters Univ. Buchhandlung, Heidelberg, Germany, Vol. 9, pp. 16–36.
- Gratacap L.P. (1916) Some minerals from Madagascar as described in Prof. A. Lacroix's *Minéralogie de la France et ses Colonies*. *American Mineralogist*, Vol. 1, No. 2, pp. 17–34.
- Guigues J. (1954) *Etude des Gisements de Pegmatite de Madagascar*, Pt. 1. Travaux du Bureau Géologique, No. 58, Service Géologique, Tananarive.
- Hawthorne F.C., Henry D.J. (1999) Classification of minerals of the tourmaline group. *European Journal of Mineralogy*, Vol. 11, pp. 201–215.
- Henn U., Bank H. (1993) Gemmologische Kurzinformationen: Turmalin-Glas-Dubletten als Querschnitte. *Gemmologie: Zeitschrift der Deutschen Gemmologischen Gesellschaft*, Vol. 42, No. 1, pp. 1–2, 4.
- Hlava P.F. (2001) Gem News International: A bismuth-bearing liddicoatite from Nigeria. *Gems & Gemology*, Vol. 37, No. 2, pp. 152–153.
- Jackson J.A., Ed. (1997) *Glossary of Geology*. American Geological Institute, Alexandria, VA.
- Johnson M.L., Koivula J.I., Eds. (1998a) Gem News: Parti-colored faceted liddicoatite tourmaline. *Gems & Gemology*, Vol. 34, No. 1, p. 54.
- Johnson M.L., Koivula J.I., Eds. (1998b) Gem News: Rossmannite, a new variety of tourmaline. *Gems & Gemology*, Vol. 34, No. 3, p. 230.
- Koivula J. (1994) The inside story. *Lapidary Journal*, Vol. 47, No. 11, pp. 56–59.
- Koivula J.I., Kammerling R.C., Eds. (1990) Gem News: Largest known faceted liddicoatite tourmaline reportedly found in Brazil. *Gems & Gemology*, Vol. 26, No. 1, p. 108.
- Koivula J.I., Kammerling R., Fritsch E., Eds. (1992) Gem News: Assembled imitation bicolor tourmaline. *Gems & Gemology*, Vol. 28, No. 3, p. 209.
- Lacroix A. (1893) *Minéralogie de la France et de ses Colonies*, Vol. 1, Pt. 1. Librairie Polytechnique, Paris.
- Lacroix A. (1908) Les minéraux des filons de pegmatite a tourmaline lithique de Madagascar. *Bulletin de la Société Française de Minéralogie*, Vol. 31, pp. 218–247.
- Lacroix A. (1910) *Minéralogie de la France et de ses Colonies*, Vol. 4, Pt. 2. Librairie Polytechnique, Paris.
- Lacroix A. (1913a) A trip to Madagascar, the country of beryls. *Annual Report of the Board of Regents of the Smithsonian Institution for 1912*, Vol. 68, pp. 371–382.
- Lacroix A. (1913b) *Minéralogie de la France et de ses Colonies*, Vol. 5. Librairie Polytechnique, Paris.
- Lacroix A. (1922a) *Minéralogie de Madagascar*, Vol. 1—Géologie, Minéralogie Descriptive. Augustin Challamel, Paris.
- Lacroix A. (1922b) *Minéralogie de Madagascar*, Vol. 2—Minéralogie Appliquée, Lithologie. Augustin Challamel, Paris.
- Lacroix A. (1923) *Minéralogie de Madagascar*, Vol. 3—Lithologie, Appendice, Index Géographique. Société d'Éditions Géographiques, Maritimes et Coloniales, Ancienne Maison Challamel, Paris.
- Laplaine L. (1951) Étude géologique des feuilles Tsiroanomandidy et Soavinandriana. *Travaux du Bureau Géologique*, No. 20,

- Service Géologique, Tananarive.
- Laurs B.M., Ed. (2001) Gem News International: More on liddicoatite from Nigeria. *Gems & Gemology*, Vol. 37, No. 3, pp. 240–241.
- Lavila L. (1923) L'industrie des pierres précieuses a Madagascar. *Bulletin des Mines de Madagascar*, No. 8, pp. 138–143.
- Malisa E., Muhongo S. (1990) Tectonic setting of gemstone mineralization in the Proterozoic metamorphic terrane of the Mozambique belt in Tanzania. *Precambrian Research*, Vol. 46, pp. 167–176.
- Menon R.D., Santosh M. (1995) The Pan-African gemstone province of East Gondwana. In M. Yoshida and M. Santosh, Eds., *India and Antarctica During the Precambrian*, Geological Society of India Memoir No. 34, pp. 357–371.
- Milisenda C.C. (2000) Plate tectonics and gemstone occurrences. In D. Rammlmair et al., Eds., *Applied Mineralogy in Research, Economy, Technology, Ecology and Culture*, A.A. Balkema, Rotterdam, The Netherlands, Vol. 1, pp. 53–55.
- Mitchell R. (1984) Particolour in tourmalines. *Journal of Gemmology*, Vol. 19, No. 1, pp. 24–26.
- Ngu P.G. (2001) Some characteristics of tourmaline in Vietnam. *Proceedings of the International Workshop on Material Characterization by Solid State Spectroscopy: Gems and Minerals of Vietnam*, Hanoi, April 4–10, pp. 265–274.
- Novák M., Selway J.B., Černý P., Hawthorne F.C., Ottolini L. (1999) Tourmaline of the elbaite-dravite series from an elbaite-subtype pegmatite at Bližná, southern Bohemia, Czech Republic. *European Journal of Mineralogy*, Vol. 11, pp. 557–568.
- Nuber B., Schmetzer K. (1981) Strukturverfeinerung von Liddicoatit. *Neues Jahrbuch für Mineralogie Monatshefte*, No. 5, pp. 215–219.
- Paquette J., Nédélec A. (1998) A new insight into Pan-African tectonics in the East-West Gondwana collision zone by U-Pb zircon dating of the granites from central Madagascar. *Earth and Planetary Science Letters*, Vol. 155, No. 1–2, pp. 45–56.
- Peters S.W. (1991) *Regional Geology of Africa*. Springer-Verlag, New York.
- Pezzotta F. (1996) Preliminary data on the physical-chemical evolution of the gem-bearing Anjanabonoina pegmatite, central Madagascar. *Program with Abstracts*, Geological Association of Canada–Mineralogical Association of Canada, Winnipeg, Manitoba, May 27–29, p. A-75.
- Pezzotta F. (2001) Madagascar—A mineral and gemstone paradise. *extraLapis English* No. 1, 97 pp.
- Pezzotta F., Franchi M. (1997) Miarolitic shallow depth pegmatites of the Betafo and Antsirabe areas, central Madagascar; genetic inferences. In R. Cox and L.D. Ashwal, Eds., *Proceedings of the UNESCO-IUGS-IGCP-348/368 International Field Workshop on Proterozoic Geology of Madagascar*, Antananarivo, August 16–30, Gondwana Research Group Miscellaneous Publication No. 5, p. 71.
- Pouchou J.-L., Pichoir F. (1985) "PAP"  $\phi(\rho Z)$  procedure for improved quantitative microanalysis. In J.P. Armstrong, Ed., *Microbeam Analysis*, San Francisco Press, San Francisco, CA, pp. 104–106.
- Sahama Th.G., von Knorring O., Törnroos R. (1979) On tourmaline. *Lithos*, Vol. 12, pp. 109–114.
- Selway J.B. (1999) Compositional Evolution of Tourmaline in Granitic Pegmatites. Ph.D. dissertation, University of Manitoba, Winnipeg, Canada.
- Selway J.B., Novák M., Hawthorne F.C., Černý P., Ottolini L., Kyser T.K. (1998) Rossmanite  $\square(\text{LiAl}_2)\text{Al}_6(\text{Si}_6\text{O}_{18})[\text{BO}_3]_3(\text{OH})_4$ , a new alkali-deficient tourmaline: Description and crystal structure. *American Mineralogist*, Vol. 83, pp. 896–900.
- Selway J.B., Novák M., Černý P., Hawthorne F.C. (1999) Compositional evolution of tourmaline in lepidolite-subtype pegmatites. *European Journal of Mineralogy*, Vol. 11, pp. 569–584.
- Shmakina B.M., Makagon V.M. (1999) *Granitic Pegmatites*, Vol. 3—*Miarolitic Pegmatites*. Nauka, Siberian Publishing Firm RAS, Novosibirsk, Russia.
- Strunz H. (1979) Anjanabonoina, Fundort schönster Turmaline. *Lapis*, Vol. 4, No. 1, pp. 24–27, 47–48.
- Teertstra D.K., Černý P., Ottolini L. (1999) Stranger in paradise: Liddicoatite from the High Grade Dike pegmatite, southeastern Manitoba, Canada. *European Journal of Mineralogy*, Vol. 11, pp. 227–235.
- Termier P. (1908) Sur de gros cristaux de tourmaline de l'Ankaratra (Madagascar). *Bulletin de la Société Française de Minéralogie*, Vol. 31, pp. 138–142.
- Webber K.L., Simmons W.B., Falster A.U. (2002) Tourmaline from the Antandrokomby, Anjanabonoina, and Fianarantsoa pegmatites, Madagascar. *Mineralogical Record*, Vol. 33, No. 1, p. 82.
- Webster R. (1994) *Gems: Their Sources, Descriptions and Identification*, 5th ed. Revised by P.G. Read, Butterworth Heinemann, London.
- Weldon R. (2000) Liddi-coat of many colors. *Professional Jeweler*, Vol. 3, No. 7, p. 46.
- Wentling J. (1980) About our cover...tourmaline—Liddicoatite. *Lapidary Journal*, Vol. 34, No. 9, p. 1918.
- Wilson W.E. (1984) What's new in minerals? Munich Show 1983. *Mineralogical Record*, Vol. 15, No. 2, pp. 117–120.
- Wilson W.E. (1989) The Anjanabonoina pegmatite, Madagascar. *Mineralogical Record*, Vol. 20, No. 3, pp. 191–200.
- Wöhrmann B. (1994) Mit Ziehfeder und Pinsel längsgeschnitten. *extraLapis* No. 6, Turmalin, pp. 24–32.
- Zagorovsky V.E., Peretyazhko I.S., Schiryevna V.A., Bogdanova L.A. (1989) Tourmalines from miarolitic pegmatites in the Malkhan Range (Transbaikalia). *Mineralogicheskii Zhurnal*, Vol. 11, No. 5, pp. 44–55.
- Zang J. (1994a) Gibt es wirklich schwarze Turmaline? *extraLapis* No. 6, Turmalin, pp. 20–23.
- Zang J. (1994b) Madagaskar's neue Konkurrenz: Zonierte Turmaline aus Sanga-Sanga, Tanzania. *extraLapis* No. 6, Turmalin, pp. 40–43.
- Zang J. (1994c) Neues vom Stern. *extraLapis* No. 6, Turmalin, pp. 32–35.
- Zang J. (1996) *101 Tourmalines*. Photo CD published by Gustav Zang, Idar-Oberstein, Germany.
- Zang J. (2000) Wachstum zonierter Turmalinkristalle aus Madagaskar [Crystal growth of color-zoned tourmaline crystals from Madagaskar]. In J. Zang, R. Dröschel, and M. Wild, Eds., *Turmalin 2000*, exhibition catalog, German Gemstone Museum, Idar-Oberstein, February 19–August 27, pp. 39–42 [English text on pp. 53–54].
- Zhdanov V.V. (1996) REE-rare metal pegmatites of Madagascar. *Proceedings of the Russian Mineralogical Society*, Vol. 125, No. 3, pp. 1–8 [in Russian].
- Zolotarev A.A., Bulakh A.G. (1999) Rossmanite, olenite, elbaite and 50% rule as a basis for distinguishing between mineral species among Li-Al tourmalines. *Proceedings of the Russian Mineralogical Society*, Pt. 128, No. 2, pp. 32–38.